MONTANA STATE UNIVERSITY

Development of artificial biofilms for use in mass transport studies
by Michael Todd Abrahamson

A thesis submitted in partial fulfillment of the requirements for the degree of Master of Science in Environmental Engineering
Montana State University
© Copyright by Michael Todd Abrahamson (1995)

Abstract:
Artificial biofilms are useful laboratory tools allowing fundamental biofilm research to be conducted under controlled and reproducible conditions. Unfortunately, these synthetic biofilms, which generally consist of uniformly distributed bacteria throughout a polymer matrix, lack the structural heterogeneity (voids, microcolonies) often seen in natural biofilms. Thus data obtained from this type of biofilm may not accurately describe the behavior of a natural biofilm system.

This thesis presents a procedure which can be used to construct an artificial biofilm that incorporates the structural heterogeneity observed in natural biofilm. Alginate was harvested from a mucoid strain of Pseudomonas aeruginosa, filter sterilized, and fixed to a glass slide where it served as the biofilm matrix. High densities of P. aeruginosa were injected into specific locations within the alginate matrix to represent microcolonies similar to those found in natural biofilms. The heterogeneous artificial biofilm was then used to study the effects of a single microcolony on the mass transport of dissolved oxygen. The artificial biofilm was probed using a dissolved oxygen microelectrode to obtain concentration profiles through the biofilm. Visual analysis of these profiles indicated that the surrounding dissolved oxygen field was affected by a single microcolony (150 μm diameter), up to a distance of 1400 μm away from the microcolony, and that the mass transfer resistance due to the biofilm matrix itself was negligible.

An artificial biofilm, containing uniformly distributed bacteria throughout an alginate matrix was used to evaluate a procedure used to extract the microbial respiration kinetics from substrate concentration profiles. Only those profiles which were partially-penetrated with respect to oxygen could be analyzed using this procedure. This indicates that the applicability of this procedure was highly dependent upon the shape of the substrate concentration profile. Those profiles which could be analyzed showed good reproducibility in determining a value for Ks. Observation of these profiles showed that the diffusion boundary layer was significantly influenced by the flow velocity. The diffusion boundary layer decreased from 0.048 cm to 0.004 cm when the flow velocity was changed from low to high.

DEVELOPMENT OF ARTIFICIAL BIOFILMS FOR USE IN MASS TRANSPORT STUDIES

by

Michael Todd Abrahamson

A thesis submitted in partial fulfillment
of the requirements for the degree

of

Master of Science

in

Environmental Engineering

MONTANA STATE UNIVERSITY
Bozeman, Montana

November, 1995

N378
Ab824

APPROVAL

of a thesis submitted by

Michael Todd Abrahamson

This thesis has been read by each member of the thesis committee and has been found to be satisfactory regarding content, English usage, format, citations, bibliographic style, and consistency, and is ready for submission to the College of Graduate Studies.

November 8, 1995
Date

Chairperson, Graduate Committee

Approved for the Major Department

November 8, 1995
Date

Head, Major Department

Approved for the College of Graduate Studies

11/17/95
Date

Graduate Dean

STATEMENT OF PERMISSION TO USE

In presenting this thesis in partial fulfillment of the requirements for a master's degree at Montana State University, I agree that the Library shall make it available to borrowers under rules of the Library.

If I have indicated my intention to copyright this thesis by including a copyright notice page, copying is allowable only for scholarly purposes, consistent with "fair use" as prescribed in the U.S. Copyright Law. Requests for permission for extended quotation from or reproduction of this thesis in whole or in parts may be granted only by the copyright holder.

Signature Michael Abrahamsen

Date November 8, 1995

ACKNOWLEDGMENTS

First I would like to express my appreciation to my academic and research advisor Dr. Zbigniew Lewandowski for his support, guidance and input in the development of my research. I would like to thank Dr. Gill Geesey and Dr. Al Cunningham for serving as members of my thesis committee. I would also like to express my gratitude to Dr. Gill Geesey for introducing me to the Center for Biofilm Engineering.

I would like to thank my wife, Stacey, for her love, support, and encouragement, and to my children, Mikaela and Kevin, whose smiles and laughter bring me happiness and keep me going.

Finally, I owe many thanks to the staff and students at the Center for their help and for making this such a rewarding research experience.

My research has been sponsored by the National Science Foundation and the Associates of the Center, my thanks to them as well.

TABLE OF CONTENTS

Page

LIST OF TABLES viii

LIST OF FIGURES ix

ABSTRACT xi

CHAPTER 1. INTRODUCTION 1

Statement of the problem 1
Goals and objectives 2

CHAPTER 2. BACKGROUND 4

Natural biofilms 4
Artificial biofilms 5
Artificial biofilm development 6
Biofilm matrix 6
Biofilm matrix preparation 9
Immobilization of microorganisms 9
Biofilm systems modeling 10
Substrate diffusivity and kinetic parameter analysis from substrate concentration profiles 15
Results of substrate diffusivity and microbial respiration kinetics reported in literature 18

CHAPTER 3. MATERIALS AND METHODS 21

Media 21
Mineral salts medium 21
Artificial biofilm medium (chemostat) 22
Artificial biofilm medium (reactor) 22
Phosphate buffer 23
YTG agar plates 23
Microorganism 24

Artificial biofilm development and construction 24
Biofilm matrix preparation 25
Polymer characterization 27
Bacterial growth conditions 28
Immobilization of microorganisms 29
Substrate transport through the biofilm 32
Dissolved oxygen microelectrode 33
Microelectrode construction 33
Microelectrode calibration 36
Experimental setup 37
Data acquisition system 38
Substrate diffusivity and microbial respiration kinetic analysis 40

CHAPTER 4. RESULTS 42

Heterogeneous artificial biofilm 42
Homogeneous artificial biofilm 44
Properties of the artificial biofilm 47
Polymer analysis 47
Substrate transport through biofilm 48
Mass transfer resistance of the biofilm matrix 49

CHAPTER 5. DISCUSSION 51

Development and characteristics of the heterogeneous artificial biofilm 51
Mode of mass transport through artificial biofilm 52
Mass transfer resistance of biofilm matrix 53
Heterogeneous biofilm application 54
Homogeneous biofilm study 56
Effects of flow velocity on mass transport 57
Oxygen diffusivity and microbial respiration kinetic analysis 61
Possible limitations of the artificial biofilm 65
Advantages and applications of artificial biofilms 66

CHAPTER 6. CONCLUSIONS 68

NOMENCLATURE 70

REFERENCES CITED 71

APPENDICES 78

Appendix A -Microelectrode reproducibility 79
Appendix B - Dissolved oxygen profiles through homogeneous artificial biofilm 82
Low flow velocity 83
High flow velocity 89

LIST OF TABLES

Table		Page
1.	Microbial extracellular polysaccharides	7
2.	Summary of respiration kinetics and oxygen diffusivities reported in literature	20
3.	Diffusivity and respiration kinetics of heterogeneous biofilm	43
4.	Diffusivity and respiration kinetics of the homogeneous artificial biofilm-low velocity	46
5.	Diffusivity and respiration kinetics of the homogeneous artificial biofilm-high velocity	46
6.	Diffusion boundary layer thickness over biofilm	47
7.	Characteristics of purified alginate from *P. aeruginosa* strain 8830	47

LIST OF FIGURES

Figure		Page
1.	Microdrop of viable bacteria in sterile alginate matrix	30
2.	Dissolved oxygen microelectrode	34
3.	Schematic diagram of experimental setup	38
4.	Procedure for extracting kinetic parameters from a substrate concentration profile	41
5.	Dissolved oxygen profiles through artificial biofilm containing a single microcolony	43
6.	Dissolved oxygen profiles through homogeneous artificial biofilm under a low velocity	45
7.	Dissolved oxygen profiles through homogeneous artificial biofilm under a high flow velocity	45
8.	Confocal images of convective transport	48
9.	Dissolved oxygen profile through sterile bacterial alginate	50
10.	Dissolved oxygen profile through sterile bacterial alginate	50
11.	Hydrodynamic and diffusion boundary layers in a biofilm system	59
12.	Dissolved oxygen profiles showing microelectrode reproducibility	81
13.	Dissolved oxygen profile (A) upstream from homogeneous artificial biofilm under a low flow velocity	83
14.	Dissolved oxygen profile (B) near homogeneous artificial biofilm under a low flow velocity	84
15.	Dissolved oxygen profile (C) through homogeneous artificial biofilm under a low flow velocity	85
16.	Dissolved oxygen profile (D) through homogeneous artificial biofilm under a low flow velocity	86
17.	Dissolved oxygen profile (E) through homogeneous artificial biofilm under a low flow velocity	87
18.	Dissolved oxygen profile (F) through homogeneous artificial biofilm under a low flow velocity	88
19.	Dissolved oxygen profile (G) downstream from homogeneous artificial biofilm under a low flow velocity	89
20.	Dissolved oxygen profile (A') upstream from homogeneous artificial biofilm under a high flow velocity	90
21.	Dissolved oxygen profile (B') near homogeneous artificial biofilm under a high flow velocity	90

22. Dissolved oxygen profile (C') through homogeneous artificial biofilm under a high flow velocity 91
23. Dissolved oxygen profile (D') through homogeneous artificial biofilm under a high flow velocity 92
24. Dissolved oxygen profile (E') through homogeneous artificial biofilm under a high flow velocity 93
25. Dissolved oxygen profile (F') near homogeneous artificial biofilm under a high flow velocity 94
26. Dissolved oxygen profile (G') downstream from homogeneous artificial biofilm under high flow velocity 95

ABSTRACT

Artificial biofilms are useful laboratory tools allowing fundamental biofilm research to be conducted under controlled and reproducible conditions. Unfortunately, these synthetic biofilms, which generally consist of uniformly distributed bacteria throughout a polymer matrix, lack the structural heterogeneity (voids, microcolonies) often seen in natural biofilms. Thus data obtained from this type of biofilm may not accurately describe the behavior of a natural biofilm system.

This thesis presents a procedure which can be used to construct an artificial biofilm that incorporates the structural heterogeneity observed in natural biofilm. Alginate was harvested from a mucoid strain of *Pseudomonas aeruginosa*, filter sterilized, and fixed to a glass slide where it served as the biofilm matrix. High densities of *P. aeruginosa* were injected into specific locations within the alginate matrix to represent microcolonies similar to those found in natural biofilms. The heterogeneous artificial biofilm was then used to study the effects of a single microcolony on the mass transport of dissolved oxygen. The artificial biofilm was probed using a dissolved oxygen microelectrode to obtain concentration profiles through the biofilm. Visual analysis of these profiles indicated that the surrounding dissolved oxygen field was affected by a single microcolony (150 μm diameter), up to a distance of 1400 μm away from the microcolony, and that the mass transfer resistance due to the biofilm matrix itself was negligible.

An artificial biofilm, containing uniformly distributed bacteria throughout an alginate matrix was used to evaluate a procedure used to extract the microbial respiration kinetics from substrate concentration profiles. Only those profiles which were partially-penetrated with respect to oxygen could be analyzed using this procedure. This indicates that the applicability of this procedure was highly dependent upon the shape of the substrate concentration profile. Those profiles which could be analyzed showed good reproducibility in determining a value for K_S. Observation of these profiles showed that the diffusion boundary layer was significantly influenced by the flow velocity. The diffusion boundary layer decreased from 0.048 cm to 0.004 cm when the flow velocity was changed from low to high.

CHAPTER 1

INTRODUCTION

Statement of the Problem

When growing biofilms in the laboratory, the researcher controls only the quality of the influent into the reactor, the kind of organism under study, the substratum material, and to a certain extent the hydrodynamic conditions of the reactor. Beyond these parameters, biofilm formation is no longer under the researchers control. One way a researcher can gain increased control over the experimental conditions, is through the use of an artificial biofilm. Artificial biofilms are useful laboratory tools, serving as simplified "models" for more complex biofilm phenomena. Artificial biofilms generally consist of uniformly distributed bacteria throughout a polymer matrix, and thus lack the structural heterogeneity (voids, microcolonies) found in some in natural biofilms. Therefore, the data obtained from this type of biofilm may not reflect the behavior of a natural biofilm system. In addition, some researchers consider cells immobilized in gel beads suspended in bulk fluid to be artificial biofilms. Because by definition "a biofilm consists of cells immobilized at a substratum..." (Characklis and Marshall, 1990), these gel beads can hardly be considered biofilm. The artificial biofilms

presented in this work were fixed to a substratum in an attempt to conform to this definition.

Goals and Objectives

The main goal of this research was to develop an artificial biofilm incorporating the structural heterogeneity seen in natural biofilm. This was accomplished through the immobilization of high bacterial densities in localized regions of a sterile matrix material, which was fixed to the substratum, to represent microcolonies. Furthermore, this artificial biofilm was compatible with microelectrode use since bacterial alginate was used for the matrix material of the biofilm. Such heterogeneous artificial biofilm would allow mass transport studies involving biofilm to be conducted under more controlled and reproducible conditions, while still maintaining some of the physical characteristics of natural biofilm. With use of this biofilm, it would be possible to produce data that more closely resembles the behavior of the natural biofilm system.

Two structurally different artificial biofilms were constructed and used in mass transport studies to demonstrate the usefulness of artificial biofilm. One contained a heterogeneous structure, the other a homogeneous structure. The heterogeneous artificial biofilm permitted the study of the effects of a single microcolony embedded in a sterile alginate matrix on the transport of dissolved

oxygen. The homogeneous artificial biofilm was used to evaluate the method currently used to extract the substrate diffusivity and microbial respiration kinetics from substrate concentration profiles. In addition the homogeneous biofilm was probed under two different flow velocities, allowing the effects of flow velocity on the microbial respiration kinetics and mass transport of oxygen to be examined.

The following objectives were set for obtaining the goal of developing artificial biofilm and evaluating their usefulness.

1) Select a biofilm matrix which was compatible with microelectode use to study the biofilm activity and mass transport.

2) Sterilize the biofilm matrix.

3) Attach the matrix to the substratum.

4) Immobilize high densities of viable bacteria into localized regions of the sterile matrix material to represent microcolonies.

5) Construct dissolved oxygen microelectrodes to monitor the transport of oxygen through the artificial biofilms.

6) Study the effects of a single microcolony embedded in a sterile alginate matrix on the transport of oxygen.

7) Evaluate the procedure currently used for the extraction of microbial respiration kinetics from substrate concentration profiles for its applicability and reproducibility.

CHAPTER 2

BACKGROUND

Natural biofilms

When nutrients in the bulk fluid become scarce, planktonic cells tend to attach to surfaces (Characklis and Cooksey, 1983 , Matilla-Sandholm and Wirtanen, 1992). Once here, these attached bacteria grow, reproduce, and excrete extracellular polymer substances (EPS) onto the surface resulting in the formation of biofilm (Characklis and Cooksey, 1983). The extracellular products are commonly polysaccharides which can be highly anionic, uronic, and acid containing polymers (Costerton, 1994). Due to their random block structure, many bacterial extracellular polymers bind large quantities of water. This makes the gel highly flexible and less susceptible to destruction by hydrodynamic forces, aiding in the survival of the microorganism (Gacesa and Russell, 1990). In addition to serving as a protective matrix, these polymers also provide cohesive forces, and adsorb nutrients for the microorganisms (Brown and Lester, 1980, Characklis and Cooksey, 1983, Matilla-Sandholm and Wirtanen, 1992).

At the microscale, the bacteria may be homogeneously distributed throughout the EPS matrix as seen in films of *Pseudomonas aeruginosa*, have an aggregated distribution as seen in films containing *Klebsiella pneumoniae*, or contain a mixture of both as seen in multiple specie biofilm (Characklis and Marshall, 1990). These observations have been supported by studies involving confocal laser microscopy. These studies have shown that the structure of some biofilm is complex and heterogeneous, containing bacterial aggregations (microcolonies) separated by interstitial voids within which the matrix is less dense. (Stoodley et al., 1994, Costerton, 1994).

Artificial biofilms

Microorganisms intentionally immobilized or entrapped in a polymer matrix layer fixed to a surface are often thought of as artificial biofilm. The construction generally consists of a polysaccharide matrix material (i.e. kelp alginate, agar, K-carageenan, etc.) into which bacteria are uniformly distributed. (Woodward, 1988, Jouenne et al., 1994, and Whitham and Gilbert, 1993). Several papers have been written which detail the procedures used for immobilizing bacteria in various types of polymers (Woodward, 1988, Smidsrød and Skjåk-Bræk, 1990). Artificial biofilms are popular for use when studying biocide and antibiotic performance against biofilm (Whitham and Gilbert, 1993, Jouenne et al., 1994).

The microbial cells in these artificial biofilms expressed similar responses as those in natural biofilm systems, showing a decreased susceptibility to biocides in comparison to planktonic cells.

Artificial Biofilm Development

Biofilm Matrix

Kelp (brown seaweed) alginate has been widely used for the immobilization of bacteria in artificial biofilms as it is commercially available, its gels are highly durable, and the technique used is considered to be mild and easy to perform (Hiemstra et al., 1983, Chen and Huang, 1988). Kelp alginate is also similar in its chemical composition to bacterial alginate which may be found in natural biofilm. Table 1 lists the types of polysaccharides produced by potential biofilm forming bacteria. Alginate is an unbranched, copolymer of 1,4 linked α-L-guluronic acids and β-D-mannuronic acid residues which occur in varying proportions and sequential arrangements (Martinsen et al., 1989, Smidsrød, 1970). The uronic acids are monosaccharides which have been oxidized at C6 to produce a carboxylate group and therefore are negatively charged. (Gacesa and Russell, 1990). The monomers can occur in homopolymeric blocks or in alternating sequences. The relative proportion of the two uronic acids varies from alginate to alginate and is a major factor in

Table 1. Microbial Extracellular Polysaccharides.(Modified from Biofilms by Characklis and Marshall, 1990)

Polysaccharide	Microorganism
Xanthan	*Xanthomonas campestris*
Dextran	*Aerobacter spp* *Streptococcus bovis* *Streptococcus viridans* *Leuconostoc mesenteriodes*
Alginates	*Pseudomonas aeruginosa* *Azotobacter vinelandii*
Gellan gum	*Pseudomonas elodea ATCC 31461*
Zanflo	*Erwinia tahitica*
Polytran	*Sclerotium glucanicum*
Pullulan	*Aureobasidium pullulans*
Curdlan	*Alcaligenes faecalis*

determining the properties of the polysaccharide (Gacesa and Russell, 1990). Alginate can be found in all kelp where it serves as a structural component of the cell wall (Cottrell and Kovacs, 1977, Smidsrød, 1974). In addition to kelp, some bacteria are able to synthesize and excrete alginate. It was observed by Linker and Jones (1966), that *Pseudomonas aeruginosa* was able to produce an alginate like polysaccharide. They later confirmed that an O-acetylated alginate was a major component of *P. aeruginosa* slime. Alginate has also been found to be

produced by the bacteria *Azotobacter vinelandii* and by several other pseudomonads. (Gacesa and Russell, 1990, Smidsrød and Skjåk-Bræk, 1990).

There are some important differences in the compositional and structural detail of bacterial alginate in comparison to the kelp alginate. The first is that kelp alginate contains poly-guluronic acid blocks (i.e. consecutive guluronic acid residues) while the alginate synthesized by *P. aeruginosa* does not. Alginate which contains guluronic acid blocks produce strong, rigid gels (Martinsen et al., 1989, Smidsrød and Haug, 1972) while alginate rich in mannuronic acid blocks, such as that produced by *P. aeruginosa,* tend to form gels that are more voluminous and elastic (Gacesa and Russell,1990, Smidsrød and Haug, 1972). The second difference is that the mannuronic acid residues are acetylated in bacterial alginate. Skjåk-Bræk et al. (1989b) determined that the acetylation of mannuronic acid residues decreases the gel strength, and increases the water binding capacity of the alginate when compared to non-acetylated kelp. The absence of guluronic acid blocks and the presence of acetylated mannuronic acid residues in the bacterial alginate results in a weaker, more flexible gel in comparison to kelp alginate (Gacesa and Russell, 1990). Use of the bacterial alginate for the matrix of the biofilm would allow the biofilm to be easily penetrated with microelectrodes without causing damage to its fragile sensing tip.

Biofilm Matrix Preparation

Several methods exist for the extraction of extracellular polymers from bacterial cultures (Brown and Lester, 1980), but not for polymer purification (i.e. removal of bacteria while maintaining polymer integrity). With use of these extraction methods (physical and chemical) the bacterial cells are separated from the polymer, usually by centrifugation, leaving the polymer dissolved in the supernatant. In this form, biochemical analyses can be performed on the polymer, but it is of little use in serving as an artificial biofilm matrix. To maintain the polymers physical integrity a filter sterilization method was developed.

Immobilization of Microorganisms

Alginate gel beads containing microorganisms are commonly used in bioreactors. They have been widely studied to determine the mass transport rate to immobilized microorganisms. Large diameter (>1 mm) kelp alginate beads containing cells, show a significant mass transport resistance of the gel matrix which often limits the reaction rates of immobilized cells (Kurosawa et al.,1989, Hiemstra et al., 1983, Ogbonna, et al. 1991, Chen and Huang, 1988). In large beads, active cells were found to a depth of only 50-200 μm (Stormo and Crawford, 1992, Kuhn et al., 1991). This corresponded to the penetration depths of oxygen for immobilized cells as well (Chang and Moo-Young, 1988). Several methods exist for improving oxygen transfer to immobilized cells and have been

classified into three groups 1) oxygenation of the bulk medium 2) use of oxygen carriers and *in situ* oxygen generation (algae cells) within the matrix and 3) immobilization of cells in microgel beads with diameters of 50-200 μm (Ogbonna et al. 1991, Kurosawa et al., 1989). To produce beads on this scale, several instruments have been developed which can make small beads from kelp alginate solutions (Stormo and Crawford, 1992, Matulovic et al. 1986, Ogbonna et al., 1991). With these instruments a solution of kelp alginate is forced through needles or nozzles of various size where vibrations or a concentric air stream shear the carrier droplets off the tip producing a fine aerosol of cell suspension which settles into a stirred solution of $CaCl_2$. These methods produce small beads 10-100 μm but most can only utilize low viscosity alginate. Due to the high viscosity of bacterial alginate, microgel beads made of this alginate can not be made using these instruments.

Biofilm Systems Modeling

To describe the mass transport of a substrate through a biofilm system, models to analyze the data generated in these systems are needed. These models can provide insight into the growth and substrate utilization kinetics within microbial films. This in turn, leads to a better understanding of biofilm processes, allowing the design and operation of reactors to be optimized (Harremoes, 1978,

Rittmann and McCarty, 1980, Muslu, 1993, Lewandowski et al., 1991). A number of different biofilm processes may be rate limiting for the overall reaction of the biofilm including the transport of nutrients from the bulk solution into and through the biofilm, the reaction itself, or the transport of by-products (Harremoes, 1978, Fan et al., 1990). The diffusivity of nutrients through the biofilm has been identified as the controlling process for the substrate uptake rate in most biofilm systems (Lewandowski et al., 1991, Kurosawa et al., 1989, Patel and Bott, 1991).

Most models tend to describe an idealized biofilm. This biofilm has a uniform cell density and thickness. Substrate concentrations change only in the z-direction normal to the surface of the biofilm. It also assumes that all required nutrients are in excess concentration, except the rate-limiting substrate. (Rittmann and McCarty, 1980, Lewandowski et al., 1991, and Hannoun and Stephanopoulos, 1986). The models commonly used to describe the behavior of a biofilm system are as follows.

Molecular diffusion, the only means of mass transport within the biofilm described above, is related to the substrate concentration by Fick's second law.

$$\left(\frac{\partial C}{\partial t}\right)_{Diffusion} = D_e\left(\frac{\partial^2 C}{\partial x^2}\right) \qquad (1)$$

where D_e is the diffusion coefficient of the substrate in the biofilm, C is the substrate concentration at the distance x from bottom of the biofilm, and t is time.

As the substrate diffuses into the biofilm, the substrate utilization at any point in the biofilm is assumed to follow a Monod relation;

$$\left(\frac{\partial C}{\partial t}\right)_{\text{Re action}} = -\frac{V_{Max}C}{K_S + C} \tag{2}$$

where

$$V_{Max} = \frac{\mu_{Max}X}{Y_{\frac{X}{S}}} \tag{3}$$

where C is the substrate concentration at the distance x from bottom of the biofilm, V_{Max} is the maximum substrate utilization rate, K_S is the half-saturation coefficient, μ_{Max} is the maximum growth rate, X is the biomass concentration, $Y_{x/s}$ is the biomass yield, and t is time.

Combining these two processes of reaction and diffusion results in the following reaction-diffusion model which can be used to describe biofilm activity;

$$\left(\frac{\partial C}{\partial t}\right)_{Biofilm} = D_e\left(\frac{\partial^2 C}{\partial x^2}\right)_f - \frac{V_{Max}C}{K_S + C} \tag{4}$$

When consumption equals transport, a steady state will occur which simplifies the equation through the removal of the partial derivatives, resulting in:

$$D_e\left(\frac{d^2C}{dx^2}\right)_{Biofilm} = \frac{V_{Max}C}{K_S + C} \tag{5}$$

Several researchers have determined the diffusivity and the rate of substrate consumption using a diffusion-reaction model similar to that in equation

(5). However, there are difficulties with this models use. The first difficulty is that this equation has no analytical solution due to the non-linear Monod-type reaction term. The second difficulty is to determine the microbial kinetic parameters and substrate diffusivity from the same experiment. In modeling studies researchers may use a numerical analysis to solve equation (5). Numerical methods are often used to give an approximate prediction and are usually calculated using algorithms on computers. With the numerical method, researchers may choose diffusivities or kinetic parameters from literature which were determined under similar experimental conditions for use in their model, (Tang and Fan, 1987, Rittmann et al., 1986, Revsbech et al., 1986) or design experiments which separate the effects of consumption (kinetic parameters) and transport (diffusion) to determine the starting parameters.

When determining the kinetic parameters of the Monod expression, batch, chemostat, or respirometry reactors with suspended cultures are generally used. This allows external and internal mass transport effects to be ignored (Fan et al., 1990). As Rittmann et al. (1986) points out, a serious drawback of the conventional chemostat or batch culture techniques used to estimate kinetic parameters for microorganisms is the possible alteration of cell physiology. The differences in kinetic parameters between suspended culture and the immobilized culture have been noticed by researchers (Fan et al. 1990, Hooijmans et al. 1990a, Hiemstra et al., 1983). For example, Toth et al. (1988) discovered that

upon encapsulation into a gel, *Escherichia coli* cells exhibit enhanced respiration. Hiemstra et al. (1983) found the apparent $K_S(O_2)$ of the immobilized cells was dependent upon the density of the cells in the alginate beads as well as the bead radius. Finally, Hooijmans et al. (1990a) conducted a study in which the intrinsic kinetic parameters of immobilized enzymes showed a decrease with a factor 2.3 for V_{Max} value and with a factor 2.7 for the K_M value when compared to the parameters for the free enzyme. Thus the immobilization process or the carrier material itself, not only can have an effect on the maximum intrinsic conversion rate (V_{Max}) but also on the affinity of the enzyme (K_M) for oxygen (Hooijmans et al., 1990a).

When determining the diffusivity of a substrate through a polymer matrix, the procedure generally used is to deactivate the biological material (biofilm) with a chemical (i.e. mercuric chloride) or use a sterilized polymer. This will allow biological kinetics to be ignored (Revsbech et al., 1986, Sun et al. 1989, Hulst et al. 1989).

Another alternative used by some is to simplify the reaction-diffusion equation by assuming zero order kinetics for which analytical solutions can be derived (Bungay et al.,1969, Rittmann and McCarty, 1980, Onuma et al., 1985, Shuler and Kargi, 1992, Larsen and Harremoes, 1994). This assumption is not without merit as the K_S values of oxygen are low in comparison to the oxygen concentrations in the dominant part of the active biofilm. The saturation constant of

oxygen (K_{ox}) for most bacteria is small (<0.5 mg/L) (Tang and Fan, 1987, Larsen and Harremoes, 1994, Chang and Moo-Young, 1988). It is not surprising that the K_S for aerobic bacteria is so low for oxygen as its value represents the affinity of the organism for the growth supporting nutrient. The lower the value the greater the bacterium's affinity for that molecule (Alexander and Skow, 1989, Wiseman, 1983).

Substrate Diffusivity and Kinetic Parameter Analysis from Substrate Concentration Profiles

As mentioned it can be difficult to obtain both the diffusivity of a substrate and microbial kinetic parameters from the same experiment. However, one way this can be achieved is with the use of microelectrodes. Microelectrodes sensitive to dissolved oxygen have seen considerable use for determining both the microbial respiration rate and diffusivity of oxygen through biofilm (Bungay et al., 1969, Revsbech et al. 1986, Hooijmans et al., 1990a, Lewandowski et al., 1991). Biofilm systems are diffusion limited, and as a result the concentration of substrates vary with depth forming concentration gradients. (Patel and Bott, 1991, Lewandowski et al., 1993). Using ion-selective and gas sensing microelectrodes with tip diameters less than 20 μm, direct measurements of these chemical gradients in biofilms can be made creating substrate concentration profiles. The

small tip allows measurements in microenvironments to be made without causing much disturbance or destruction to the biofilm structure. As Lewandowski (1994) states, the shape of the profile is simultaneously influenced by these three factors:

1 - microbial substrate uptake rate which is a function of microorganism concentration and their affinities for the substrate,

2 - substrate transport rate through the film which depends on substrate diffusivity through the biofilm, and

3 - substrate transport rate to the biofilm which is a function of microbial substrate uptake rate, substrate diffusivity through the water, and hydrodynamics near biofilm surface.

A major advantage of using microelectrodes is the ability to obtain data normally not available such as detailed chemical analysis of the bulk water as well as chemical measurements inside the biofilm (Lewandowski, 1994). Another advantage of using microelectrodes includes its fast response and the reduction of very small amounts of oxygen making measurements in stagnant medium possible, such as that found in biofilm (Revsbech and Ward, 1983, Hooijmans et al., 1990b).

The mass transport coefficient and kinetic parameters for oxygen in the artificial biofilm can be determined from substrate concentration profiles using a procedure developed by Lewandowski et al. (1991). With this procedure, a dissolved oxygen microelectrode is used to measure the dissolved oxygen

concentration above and along the depth of the biofilm. The biofilm-water interface is located on the substrate concentration profile allowing the profile to be divided into two parts: the bulk, which contained information about substrate transport to biofilm, and in the biofilm, which contained information about the microbial activity (Lewandowski et al., 1991). Using a microprobe, which simultaneously measured the substrate concentration and optical density, Lewandowski et al. (1991) were able to show that the interface can be located where a discontinuity (inflection point) occurs in the substrate concentration profile. The discontinuity arises because the mass transfer of substrate in the water and the biofilm are governed by different equations that are tied together by the requirement that the substrate flux at the biofilm-water interface be continuous at a steady state. The external mass transport resistance (bulk fluid profile) was modeled by the following empirically derived equation:

$$\frac{C - C_s}{C_b - C_s} = 1 - Exp[-A(x - x_s)] \qquad (6)$$

where C is the local substrate concentration, C_s is the substrate concentration at the surface of the biofilm; C_b is the substrate concentration in the bulk fluid, x is the distance from bottom of the biofilm, x_s is the biofilm thickness, and A is an experimental coefficient determined graphically from the slope of a linearized form of equation (6).

The profile in the biofilm was described using a third order polynomial regression and modeled using equation (5) and its integrated form

$$\left(\frac{dC}{dx}\right)_{Film} = \sqrt{2\frac{V_{Max}}{D_f}(C - C_o - K_S \ln\frac{K_S + C}{K_S + C_o})} \quad (7)$$

where C is the substrate concentration at a distance x from bottom of the biofilm, C_o is the substrate concentration at the substratum, D_f is the diffusion coefficient for the substrate in the biofilm, V_{Max} is the maximum substrate utilization rate, K_S is the half-saturation coefficient.

The advantages of using this technique is that it does not require extensive sample preparation, simplifying assumptions, (Lewandowski, 1991) nor a time rate of change measurements as many other techniques do (Bungay et al., 1969, Sanders et al., 1970).

Results of Substrate Diffusivity and Microbial Respiration Kinetics Reported in Literature

A summary of the kinetic parameters and diffusivities found in biofilm and 'artificial biofilm' using different procedures are presented in Table 2. As seen in Table 2 a wide range of diffusivities have been reported in literature using similar polymers. The diffusion coefficients of solutes in gels are often inconsistent and can seldom be compared with one another, in part due to the considerable variations in the experimental conditions that are used. (Martinsen et al., 1992, Ruiz-Bevia, et al., 1989). The diffusivities of various substrates through biofilm vary

from as low as 2% to as high as 122% of the molecular diffusivity in water. Several factors have been shown to have an effect on the diffusivity of a solute through biofilm. Among these factors are a biofilm's structure, cell density, amount of extracellular compounds present, age, and roughness of the surface, which increases the mass transfer into the biofilm near the surface (Tang and Fan, 1987, Fan et al., 1990, Siegrist and Gurjer, 1985). Furthermore, there are also inherent inaccuracies in the experimental methods used. For example, the change in substrate concentrations through the film is not simply a mass transfer effect, but it is also being consumed by the cells in the biofilm. It is difficult to separate these effects and estimate the contributions due to mass transfer resistance and substrate consumption (Patel and Bott, 1991). Finally, as Hulst et al. (1989) points out, the differences seen in the effective diffusivity through purified polymer matrices may be due to the degree of gel inhomogeneity. It was shown by Skjåk-Bræk et al. (1989a) that alginate gels have neither a homogeneous polymer concentration nor structure throughout them due to the kinetics of gel formation.

Table 2. Summary of respiration kinetics and oxygen diffusivities reported in literature.

Matrix Material / Method of Analysis	Oxygen Half-Saturation Coefficient (K_S)	Oxygen Utilization Rate	Oxygen Diffusivity Through Matrix $\left(\frac{D_{Matrix}}{D_{Water}}\right)\times 100\%$	Reference
Biofilm / Microelectrode	0.25 mg/L	0.05 mg/L-s	88	Lewandowski et al. (1991)
Biofilm / Microelectrode	0.025 mg/L	0.037 mg/L-s	66	Lewandowski (1994)
Biofilm / Microelectrode - Reactor	ND	0.17 mg/L-s	122	Larsen and Harremoes (1994)
Biofilm / Microelectrode	ND	0.025 mg/L-s	2-5	Bungay et al. (1969)
Biofilm / Microelectrode	ND	ND	51	Revsbech (1989)
Biofilm / Microelectrode	ND	0.34 mg/L-s	33	Chen and Bungay (1981)
Alginate Bead / Diffusion model	ND	ND	54-76	Hulst et al. (1989)
Agar Bead/ Microelectrode	0.57 mg/L	0.158 mol/kg-s	80 (Literature)	Hooijmans et al. (1989)
Alginate Bead / Reactor - Diffusion Model	0.15 to 0.768 mg/L	3.5 to 13.3 mmol/g cell-h	88-99	Kurosawa et al. (1989)
Alginate gel / Diffusion Cell	ND	ND	84-86	Sun and Furusaki (1988)
Agar gel / Diffusion Cell - Reactor	0.075 mg/L (Batch Reactor)	0.135 mg/L-s	70	Sato and Toda (1983)
Biological Aggregates / Diffusion Cell	ND	ND	20-100	Matson and Characklis (1976)

ND - Not Determined. Experiments used zero-order kinetics or deactivated biofilm.

CHAPTER 3

MATERIALS AND METHODS

Media

The following media were used in association with work on the artificial biofilm and will be made reference to in this chapter.

Mineral Salts Medium

(grams/Liter)

K_2HPO_4, 7.0; KH_2PO_4, 3.0; $(NH_4)_2SO_4$, 1.0; $MgSO_4 \cdot 7H_2O$, 0.1; Glucose, 2.0; Distilled H_2O, 1 Liter. [pH 7.2.]

Preparation:

1) Add phosphates to 500 mL of distilled water. In a separate flask add sulfates to 500 mL distilled water. Autoclave phosphates and sulfates solutions for 25 min at 20 psi pressure 121 °C.
2) Let solutions cool to 25 °C and aseptically combine.
3) Filter sterilize glucose into combined solution. Mix thoroughly.

Artificial Biofilm Medium (Chemostat)

(grams/Liter)

Glucose, 1.00; $(NH_4)_2SO_4$, 0.15; $MgSO_4 \cdot 7H_2O$, 0.10; 3-phosphoglyceric acid, 0.05; L-histidine, 0.01; CaCl2, 3.68 (50 mM); Tris(hydroxymethyl)aminomethane, 10.0; Distilled H_2O, 1 Liter.

Preparation:

1) Add all components (except glucose and 3-phosphoglyceric acid) to distilled water. Mix thoroughly.
2) Adjust the pH to 7.2 using concentrated HCl.
3) Autoclave (10 Liters) for 60 min at 20 psi pressure 121 °C.
4) Let solution cool to 25 °C. Filter sterilize glucose and 3-phosphoglyceric acid into autoclaved solution. Mix thoroughly.

Artificial Biofilm Medium (Reactor)

(milligrams/Liter)

Glucose, 75.0; $(NH_4)_2SO_4$, 7.50; $MgSO_4 \cdot 7H_2O$, 5.00; 3-phosphoglyceric acid, 2.50; L-histidine, 0.01; CaCl2, 3.68 (50mM); Tris(hydroxymethyl)aminomethane, 10.0; Distilled H_2O, 1 Liter.

Preparation:

1) Add all components (except glucose and 3-phosphoglyceric acid) to distilled water. Mix thoroughly.

2) Adjust the pH to 7.2 using concentrated HCl.

3) Autoclave (10 Liters) for 60 min at 20 psi pressure 121 °C.

4) Let solution cool to 25 °C. Filter sterilize glucose and 3-phosphoglyceric acid into autoclaved solution. Mix thoroughly.

Phosphate Buffer

(grams/Liter)

Na_2HPO_4, 0.4; KH_2PO_4, 0.2; Distilled H_2O, 1 Liter. [pH7.2]

Preparation:

1) Add components to distilled water. Mix thoroughly.

2) Autoclave for 30 min at 20 psi pressure 121 °C.

3) Aseptically fill sterile test tubes (25 mL) with 9.0 mL of cooled buffer.

YTG Agar Plates

(grams/Liter)

Yeast Extract, 5.0; Tryptone, 10.0; Glucose, 2.0; Agar, 15.0; Distilled H_2O, 1 Liter.

Preparation:

1) Add all components to distilled water. Mix thoroughly.

2) Autoclave for 35 min at 20 psi pressure 121 °C.

3) While solution is still molten pour 25 mL into sterile petri dish.

4) Agar will solidify when cooled. Store cooled plates in plastic bag.

Microorganism

The microorganism used for both the production of alginate and immobilization was *Pseudomonas aeruginosa* strain 8830. Strain 8830 is a stable alginate-producing organism derived from strain 8821, a non-stable mucoid isolate from the sputum of a cystic fibrosis patient (Darzins and Chakrabarty, 1984). This organism provides a reliable means of obtaining large volumes of bacterial alginate needed for the matrix of the biofilm. Members of the genus *Pseudomonas* are classified as motile (polar flagella), gram negative rods that are 0.5-1.0 μm in diameter by 1.5-5.0 μm in length. They grow at temperatures in the mesophilic range, and are aerobic, having a strictly respiratory type of metabolism with oxygen as a terminal electron acceptor. In some cases nitrate can be used as an alternative electron acceptor allowing growth to occur anaerobically (Bergey et al., 1984).

Artificial Biofilm Development and Construction

Two types of artificial biofilm were constructed, one containing a heterogeneous structure, the other a homogeneous structure. The artificial biofilm with a heterogeneous structure (microcolonies) was used to study the effects of a single microcolony on the transport of dissolved oxygen. The

primary use of the homogeneous artificial biofilm was to evaluate the method currently used to extract the substrate diffusivity and microbial respiration kinetics from substrate concentration profiles. Use of a homogeneous artificial biofilm enabled several profiles to be easily generated for analysis. Because this biofilm was probed with a microelectrode under both low (0.04 cm/s) and high (2.75 cm/s) flow velocities, its secondary use was to see what effects velocity may have on the microbial respiration kinetics and mass transport of oxygen. Both biofilms were composed of the same materials, with the only difference being the way in which the microorganisms were immobilized.

Biofilm Matrix Preparation

With the selection of bacterial alginate for use as the artificial biofilm matrix it was necessary to inactivate the bacteria which produced the alginate. This allowed for a controlled distribution of bacteria throughout the biofilm matrix material. Heating methods were tried for the sterilization of the bacterial alginate. However, these methods of sterilization exposed the alginate to high temperatures, bringing about the possibility of alginate degradation. In addition considerable cell disruption would occur resulting in the contamination of the polymer by intracellular material of lysed cells (Rudd et al., 1984). To avoid such problems, the following filter sterilization method was developed.

Pseudomonas aeruginosa 8830 was grown in batch culture on a Mineral Salts Medium, as previously described. When the batch culture became turbid,

several spread plates of this organism were made on yeast, tryptone and glucose (YTG) agar plates. These plates were incubated at room temperature for several days after which a uniform layer of alginate covered the entire plate. The alginate was removed from the agar plates using the edge of a microscope slide to gently scrape the surface gathering the alginate. This conglomerate of alginate and bacteria, which was too viscous to be directly filtered, was transferred to a test tube and diluted with distilled water (10:1). This slurry was homogenized using a tissumizer (Tekmar Company, Cincinnati, OH) and centrifuged (RC5C Sorvall Instruments, Du Pont Company, Wilmington, DE) at 20,000 rpm for 20 minutes. The supernatant was transferred to another tube and the pellet of bacteria was discarded. The tissumizer/centrifugation step was repeated to remove any remaining bacteria from the supernatant. The supernatant was then filtered through a 0.2 μm filter (Cole-Parmer, Niles, IL) into a sterile test tube. Excess water was removed from the diluted alginate with a HBI standard rotary evaporator (Model 421-1655, Buchler Instruments, Lenexa, MO). The evaporator was run until the alginate formed a gel that had a similar consistency as originally produced by the bacteria on the agar plates. The sterile alginate was used as the matrix material of the artificial biofilm, entrapping bacterial cells, after checking for microbial contamination by plating a 0.1 mL aliquot onto YTG agar plates.

Polymer Characterization

The extracellular polymer produced by *Pseudomonas aeruginosa* strain 8830 was characterized by ^{1}H-NMR. Since this instrumentation was not available at this research facility, the work was performed at the Norwegian Biopolymer Laboratory located at the University of Trondheim, Norway, under the direction of Dr. Bjørn E. Christensen. The procedure was as follows. Cells were diluted in saline and centrifuged. The supernatant was divided into two parts of approximately the same volumes. The first part was dialyzed exhaustively against MQ-water. The bacterial alginate was precipitated by adding isopropanol (50% v/v). The alginate was further washed with 70% ethanol and then 96% ethanol, and finally with diethylether before air drying. The second part of the supernatant was treated with 0.1 M NaOH at room temperature for 20 min. to remove O-acetate groups bound to the D-mannuronic acid residues of the alginate. Following neutralization, the deacetylated alginate was precipitated, as described above, except that ethanol replaced isopropanol in the first step.

The native and deacetylated alginates were subjected to a slight depolymerization before analysis by NMR. This involved mild acid hydrolysis at pH 5.6 for 60 min, followed by hydrolysis at pH 3.8 for 60 min. The temperature was 100° C. The pH was then adjusted to 6.8, and the material was freeze-dried. The chemical composition and sequential parameters were determined by ^{1}H-NMR analysis as described by Grasdalen (1983).

Analytical HPLC-LALLS experiments were performed using three serially connected columns (TSK G6000-PWXL, G5000-PWXL and G4000-PWXL) and eluted at 0.5 mL/min at ambient temperature with 0.05 M Na_2SO_4 containing 0.01 M EDTA (pH 6). Injection volumes were 50 mL with polysaccharide concentrations in the range 0.4 - 1 mg/mL. Light scattering data (Chromatix KMX-6 light scattering photometer equipped with the standard HPLC flow cell) and refractive index data (Shodex RI SE-61 detector) were collected and analyzed by the PCLALLS software, which also controlled the autoinjector (Shimadzu SIL-10A).

Bacterial Growth Conditions

The bacteria selected for immobilization in the alginate matrix was *Pseudomonas aeruginosa* strain 8830. This organism was grown in a 500 mL chemostat with a 16 hour residence time at 23 °C. The Artificial Biofilm Medium (Chemostat), was used to culture the bacteria in the chemostat. A chemostat was utilized so that the immobilized bacteria were always at the same physiological state. After a steady state in the chemostat had been achieved (minimum 3 residence times) 1 mL of the bulk fluid was removed and serial dilutions in phosphate buffer were made and plated onto YTG agar plates. This not only quantified the steady state population of bacteria in the chemostat, but also checked for the presence of any contaminating microorganisms as well.

The remainder of the bulk fluid was centrifuged at 10,000 rpm for 15 minutes to pellet the cells.

Immobilization of Microorganisms

Heterogeneous Biofilm - A layer of the sterile bacterial alginate (1.0 cm X 1.0 cm X 0.11 cm) was fixed onto the glass bottom of the reactor. This was accomplished by drying a thin film of sterile, medium viscosity, kelp alginate solution (3% w/v) (Sigma Chemical Co., St. Louis, MO) onto the glass slide in the reactor and then overlaying it with the sterile bacterial alginate. The pellet of cells (10^{10} CFU) from the chemostat was suspended uniformly into 0.5 mL of sterilized alginate. A microdrop (1.80 nL) of the bacteria/alginate suspension was injected into the artificial biofilm matrix by a micropipette. The micropipette, with a tip opening of 20 μm, was made from a 1 mm glass capillary tube (World Precision Instruments, Inc, New Haven, CT) using a microelectrode puller (Stoelting Co., Wooddale, IL.). The alginate/bacteria suspension was introduced into the micropipette using a syringe equipped with a 25 gauge needle. The tip of the micropipette was completely filled with the suspension to avoid injecting air bubbles into the matrix. The micropipette was mounted on a micromanipulator (Model M3301R, World Precision Instruments, New Haven, CT) that was equipped with a stepper motor (Model 18503, Oriel, Stratford, CT) and manipulated by a computer controller (Model 20010, Oriel, Stratford, CT). The tip of the micropipette was lowered into the sterile alginate with the use of the

micromanipulator to the desired depth. The viscous bacteria/alginate slurry was forced through the micropipette using compressed air. The size of the bead was monitored using bright field microscopy (10X objective) through an inverted microscope (IMT-2, Olympus, La Palma, CA) equipped with a scale in the eyepiece. When the bead reached the desired size of 150 μm the air supply to the micropipette was quickly stopped and the micropipette removed from the alginate matrix leaving a spherical microdrop (Figure 1). The microdrop was similar to the cell clusters found in natural biofilms.

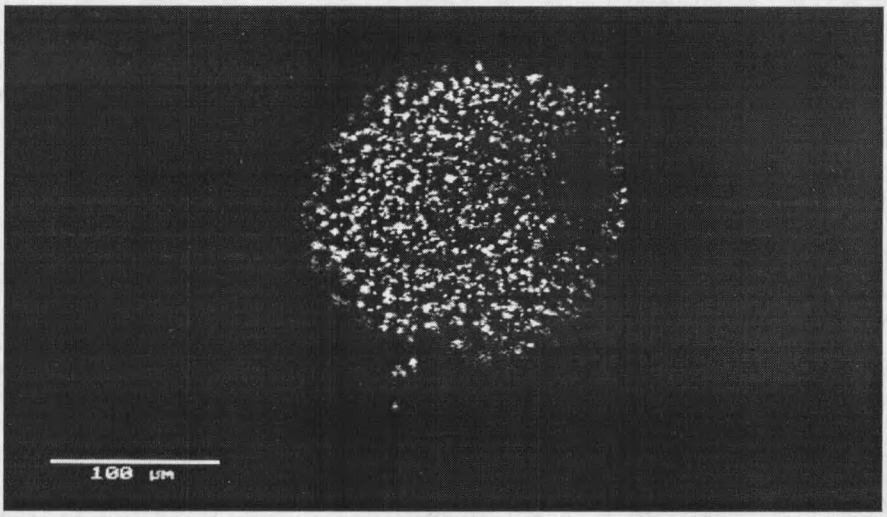


Figure 1. Microdrop of viable bacteria in sterile alginate matrix. The bacteria, which were stained using a 0.1 ppm ethidium bromide solution, appear white, while the sterile alginate matrix appears black.

After immobilizing the microorganisms, the Artificial Biofilm Medium (Reactor) was gravity to the reactor (see Figure 3). This medium contained a background of calcium chloride (25 mM) which was needed to stabilize the

artificial biofilm in the reactor. Without its presence the biofilm would lose mechanical stability and wash away. The flow of the bulk fluid through the reactor's flume had a depth of 1.0 cm and was laminar (Reynolds number (Re) =112) with an average flow velocity of 2 cm/s. The temperature of the fluid was maintained at 25 °C. The flow of medium through the reactor ran for 3 hours before probing with a dissolved oxygen microsensor.

Homogeneous Biofilm -The pellet of cells (10^{10} CFU) from the chemostat was suspended uniformly into 0.5 mL of the sterilized alginate. A thin film of 3% kelp alginate, was dried on the surface of the reactor. The homogeneous artificial biofilm (1 cm X 2 cm X ~0.04 cm) was created by covering this kelp alginate layer with 0.1 mL of the bacteria/alginate suspension.

After construction of the homogeneous artificial biofilm was completed, the Artificial Biofilm Medium (Reactor), was gravity fed to the reactor (see Figure 3). The velocity of the fluid to the reactor was controlled using tubing of different diameter. Measurements with a dissolved oxygen microelectrode were first made under a low flow velocity (tubing size 2 mm ID). The bulk fluid, based on a flow discharge, had an average flow velocity of 0.04 cm/s at 22 °C. The flow depth in the flume was 1.5 cm and characterized as being laminar (Re=2.4). The medium to the reactor, at this flow velocity, ran for 1 hour before probing began. After completing the collection of data under the low flow velocity, the same biofilm was used to collect data under a high flow velocity. The velocity through the reactor was increased by replacing the tubing which connected the upper

reservoir to the reactor with a larger diameter tubing (5 mm ID). The bulk fluid, based on a flow discharge, had an average flow velocity of 2.75 cm/s at 22 °C. The flow depth was 1.0 cm and was characterized as being laminar (Re=138). Again, the flow of medium through the reactor was run for 1 hour before any probing with a dissolved oxygen microelectrode occurred.

Substrate Transport Through the Biofilm

A dye tracer study was conducted to see if molecular diffusion or if convective flow is the dominant mode of transport through the artificial biofilm. An 800 μm sterile bacterial alginate layer was fixed to the bottom of an open channel reactor. A nanoliter pump (Model A1400, World Precision Instruments, Sarasota, FL) equipped with a micropipette (tip diameter 20 μm) was used to deliver fluorescein (5mM) to specific locations within the bulk fluid and alginate layer. A small volume of fluorescein was continuously injected into the bulk aqueous phase under both stagnant and flowing medium (3 cm/s) conditions. A motor driven micromanipulator was then used to lower the micropipette into the alginate layer where fluorescein was again continuously injected under the two flow conditions previously mentioned. The alginate and fluorescein plume were visualized using confocal microscopy (BioRad MRC600 in conjunction with an Olympus BH2 light microscope, 20X objective). If a plume formed in the direction of flow within the alginate layer, convective flow was occurring.

Dissolved Oxygen Microelectrode

A Clark-type oxygen microelectrode (Figure 2) as described by Jørgensen and Revsbech (1988) was constructed. This probe was used to determine the concentration gradient of oxygen through the artificial biofilm. The probe consisted of an outer casing that housed both a single cathode and a silver/silver chloride (Ag/AgCl) reference electrode. The configuration of this probe resulted in less electrical interference producing data that was easier to analyze and interpret. A second advantage with use of the this type of electrode is that the inner components of the probe were separated from the bulk aqueous environment by a silicone membrane. This membrane allowed dissolved oxygen to pass through it, but not ions such as calcium and magnesium; which can influence the current of the probe (Hooijmans et al., 1990b). Due to the requirement of calcium in the medium to stabilize the biofilm, the Clark-type microelectrode must be used when collecting data in the artificial biofilm. The microelectrode profile reproducibility can be seen in Appendix A.

Microelectrode Construction

The outer casing was made from borosilicate glass tubing O.D. 6 mm. The borosilicate tubing was put through a series of pulls. The first pull was done by heating the tube over a propane torch and pulling on the ends of the tube by hand. The second and third pulls were made using a microelectrode puller equipped with

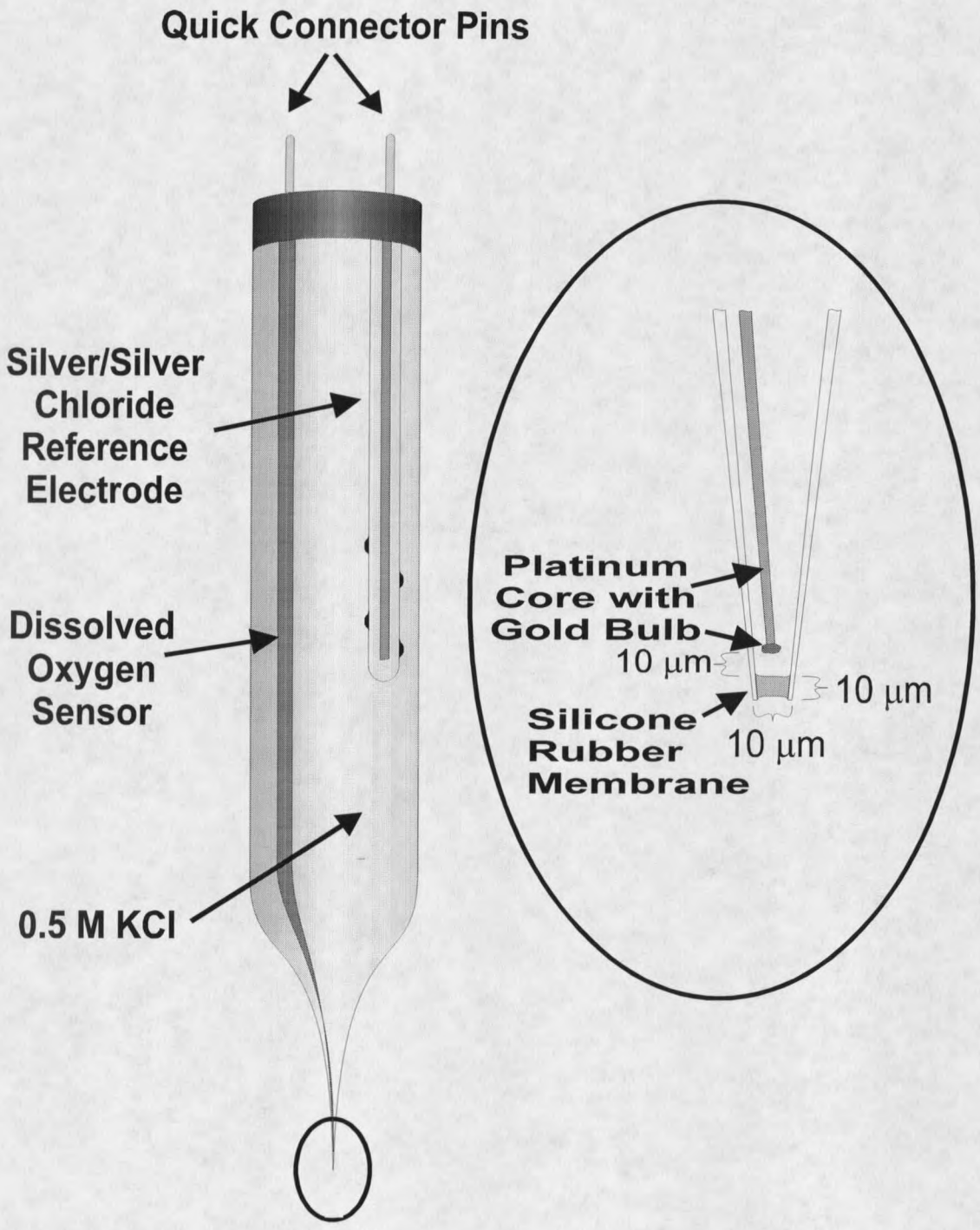


Figure 2. Dissolved oxygen microelectrode.

a 1500 μm and 100 μm diameter heating element respectively. This series of pulls produced an outer casing tip diameter of 10 μm. This tip, which is open, was filled with uncured silicone, by capillary suction, to a depth of 10-15 μm and allowed to dry for 24 hours. The single cathode was made from a 0.1 mm high purity (99.99%) platinum wire (Engelhard, Carteret, NJ) with one end etched electrochemically (7 Volts AC) in 2M KCN solution to a diameter of about 5 μm. The wire was rinsed with distilled water and dried. This wire was then carefully inserted into a soda-lime glass capillary tube and a copper lead soldered to it. The tip of the etched wire was located under a microscope and marked. The glass capillary was placed in a microelectrode puller with the tip of the wire 1.5 cm above the Ni-Cr heating element. As the glass capillary tube was heated, it began to melt, completely coating the platinum wire with a thin layer of glass. The tip of the platinum wire was exposed by grinding on a rotating diamond wheel (Model EG-4, Narishigen Co., Tokyo, Japan). The glass surrounding the polished tip was melted back exposing 3-5 μm of the platinum wire. This exposed platinum was coated with a thin layer of gold by electrochemical plating. This was done by immersing the tip of the cathode into a 5% solution of $KAu(CN)_2$ and applying 4 volts, supplied by a DC voltage source, for 1 to 2 seconds.

The Ag/AgCl reference electrode was made by first immersing 6 cm of a 0.5 mm diameter, 99.99% pure silver wire into concentrated nitric acid to clean the

surface. The silver wire was then placed into 0.1 HCl and a current density of 0.4 mA/cm^2 was applied for 1 hour until the wire was uniformly coated with a layer of AgCl. A carbon bar was used to complete the circuit. The electrode was rinsed thoroughly in distilled water and then inserted into a 4 inch glass capillary tube. The capillary tube was equipped with two holes for electrolyte transport to the reference. The glass capillary tube prevents the particles of the silver chloride from peeling off from the silver wire and depositing at the tip.

Viewed through a microscope, the cathode was carefully inserted into the outer casing using a micromanipulator until the tip of the cathode was 10 μm from the silicone membrane. The cathode was glued into place using a 24 hour epoxy. The reference electrode was placed into the outer casing as well, but not glued. This enabled the reference electrode to be cycled amongst different electrodes. The circuit was completed with a 0.5 M KCl electrolyte filling solution.

Microelectrode Calibration

Before use, the electrode was calibrated under conditions (medium and temperature) similar to those found in the reactor. This was done by taking 500 mL of the medium from the reactor and aerating it for several minutes. The tip of the electrode was then immersed into the aerated medium and the current measured using a picoammeter. This determined the current associated with oxygen saturated concentrations. The same medium was then purged with

nitrogen to remove oxygen from the medium. The current was then measured again, this time determining the current associated with nitrogen saturated (zero oxygen) concentrations. All probes used in this research expressed an oxygen current which was a least five times higher than the nitrogen current. This calibration curve, which is assumed to be linear, was then used to determine the dissolved oxygen concentrations from the recorded data collected by the picoammeter.

Experimental Setup

The experimental setup shown in Figure 3 was used for both the heterogeneous and homogeneous artificial biofilm studies. The custom-made, open channel reactor (10) was constructed from polycarbonate and contained a glass window located at the bottom of the channel. The glass window allowed the biofilm to be viewed from below using an inverted microscope (9), while still allowing easy access by the microelectrode (3) from above. The flume of the reactor was 2 cm wide and had a liquid entrance length of 20 cm to the point of the measurements.

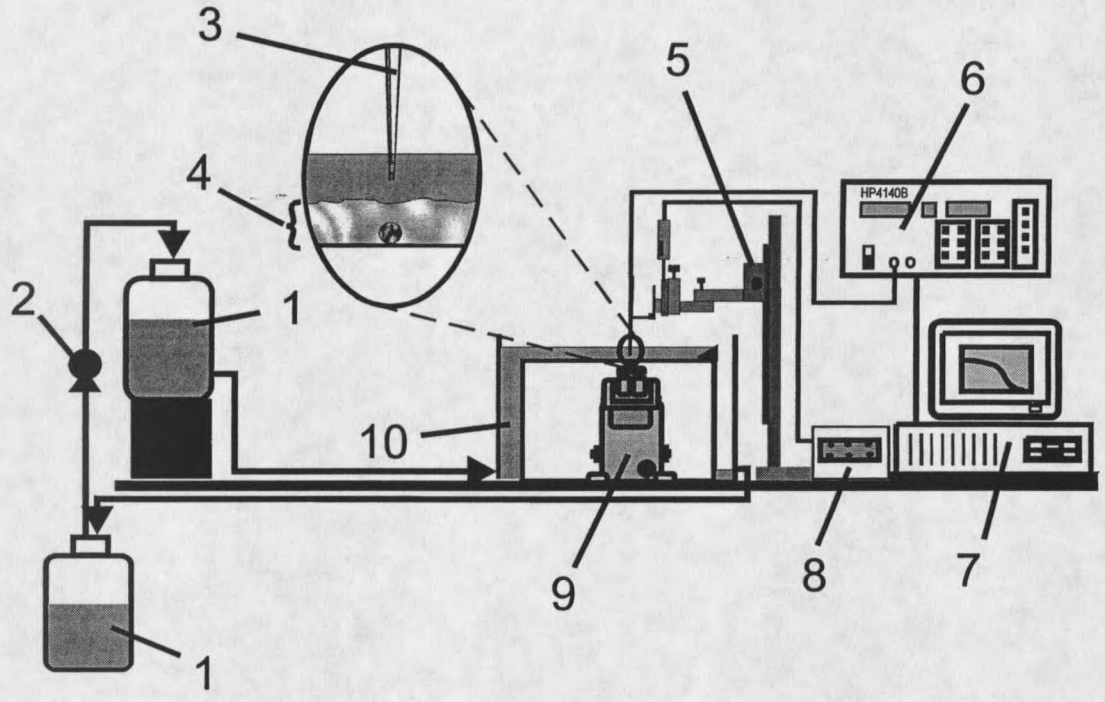


Figure 3. Schematic diagram of experimental setup. 1) Upper and lower medium reservoirs 2) Pump 3) Dissolved oxygen microelectrode 4) Artificial biofilm 5) Micromanipulator 6) Picoammeter 7) Data acquisition system 8) Controller 9) Inverted microscope 10) Open channel reactor

Data Acquisition System

The microelectrode was mounted to the motor driven micromanipulator (5), and moved vertically through the biofilm in predetermined increments. The movement of the micromanipulator was controlled by the computer (7) and stepper motor which allowed precise steps of 10 μm to be made through the biofilm. A Hewlett Packard 4140B multimeter (6) was used to apply a polarizing voltage and serve as a picoammeter to measure current. The cathode of the microelectrode was polarized (-0.8 V) against the internal Ag/AgCl reference

electrode. When oxygen diffused through the silicone membrane, it was reduced at the cathode, resulting in a flow of electrons that was detected as a current by the ammeter. This current was proportional to the concentration of dissolved oxygen present at a localized region in the biofilm (Hooijmans et al., 1990b).

The computer contained a custom-made software program that recorded the magnitude of the current and the accumulated distance the probe had moved. At each step, the software program collected 22 separate current readings at a sampling frequency of 1 Khz. The high and low values were rejected and the remaining 20 measurements were averaged. A standard deviation was determined for each set of 20 measurements and compared with a preset standard deviation. If the measured standard deviation was smaller than the preset standard deviation, the measurement was accepted and stored by the computer. If the measured standard deviation was greater than that which was preset, the measurement was repeated until an acceptable value was reached. A standard deviation of 5% was set for all measurements. This program also displayed the dissolved oxygen profiles in real time. This made it possible to visually monitor the development of each profile during the experiment and easily detect experimental problems. All experiments were completed within 6 hours after inoculating the reactor with the biofilm.

Substrate Diffusivity and Microbial Respiration Kinetics Analysis

Figure 4 is an outline of the procedure used to determine the substrate diffusivity and microbial respiration kinetics (V_{Max} and K_S), of the biofilm from substrate concentration profiles. The details of this procedure have been described by Lewandowski (1994). With this procedure the precision of the solutions (kinetic parameters and diffusivity) obtained are directly related to the precision with which the biofilm-water interface can be located. The position of this interface was located on the dissolved oxygen concentration profile using the inverted microscope. The biofilm thickness was found by focusing on the biofilm-bulk water interface and recording the distance traveled by the probe tip until it reached the bottom of the reactor. The substrate concentration profile was separated at the interface and analyzed. The external mass transport resistance (bulk fluid profile) was modeled using equation (6). The activity of the biofilm (oxygen profile in biofilm) was described using third and fourth order polynomials and modeled by equations (5) and (7).

The following assumptions were made in applying these models to data taken in the artificial biofilm. 1) cell density was uniform throughout the biofilm in space and time, 2) diffusion in the biofilm followed Fick's second law 3) molecular diffusivity of oxygen was constant in the biofilm 4) the system was

considered to be at steady state 5) oxygen was the only limiting nutrient and 6) oxygen uptake followed Monod kinetics.

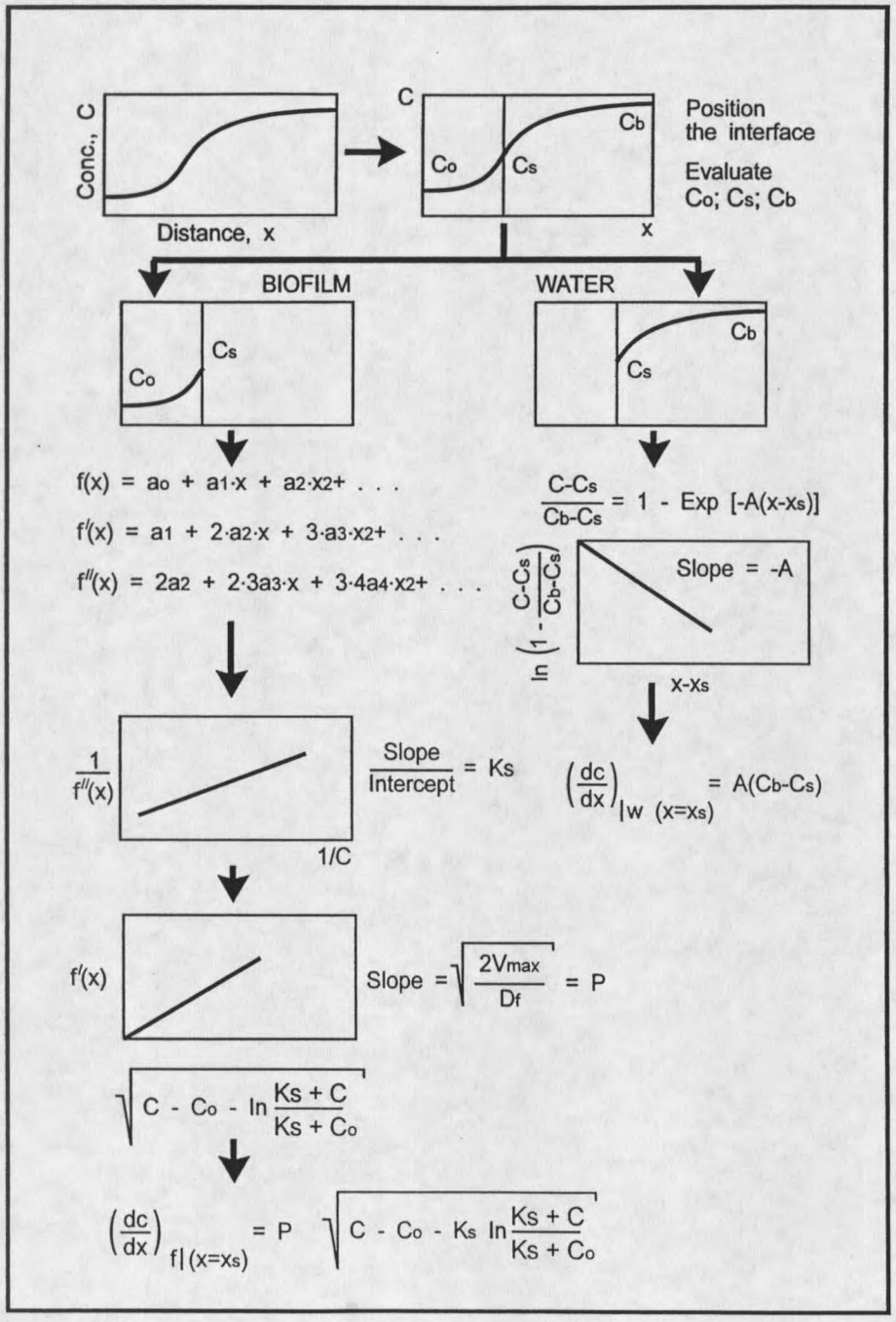


Figure 4. Procedure for extracting kinetic parameters from a substrate concentration profile (Modified from Lewandowski et al., 1994).

CHAPTER 4

RESULTS

Heterogeneous Artificial Biofilm

A procedure has been developed for creating an artificial biofilm which incorporated some of the structural heterogeneity seen in natural biofilm. This artificial biofilm was composed of bacterial alginate and contained a 'microcolony' which was on the same scale as those found in natural biofilm.

Figure 5 shows ten dissolved oxygen profiles taken through this artificial biofilm. The microcolony had a 0.015 cm diameter with a density of 10^{10} CFU/ mL alginate. The base of the biofilm was located at x = 0 cm. The average flow velocity over the biofilm was 2.0 cm/s. The alginate-water interface was located at 0.12 cm. The dissolved oxygen concentration above this interface was constant throughout the bulk fluid at 6.8 mg/L. Below this interface a decrease in the oxygen concentration was observed in profiles (A - J). Profile (A) was taken through the microcolony. The surface of the microcolony was located at approximately 0.015 cm on this profile. Profiles (B - J) were taken through the sterile alginate matrix at various distances adjacent to the microcolony. The distance of each microcolony from the center of the microcolony is shown in the legend of Figure 5.

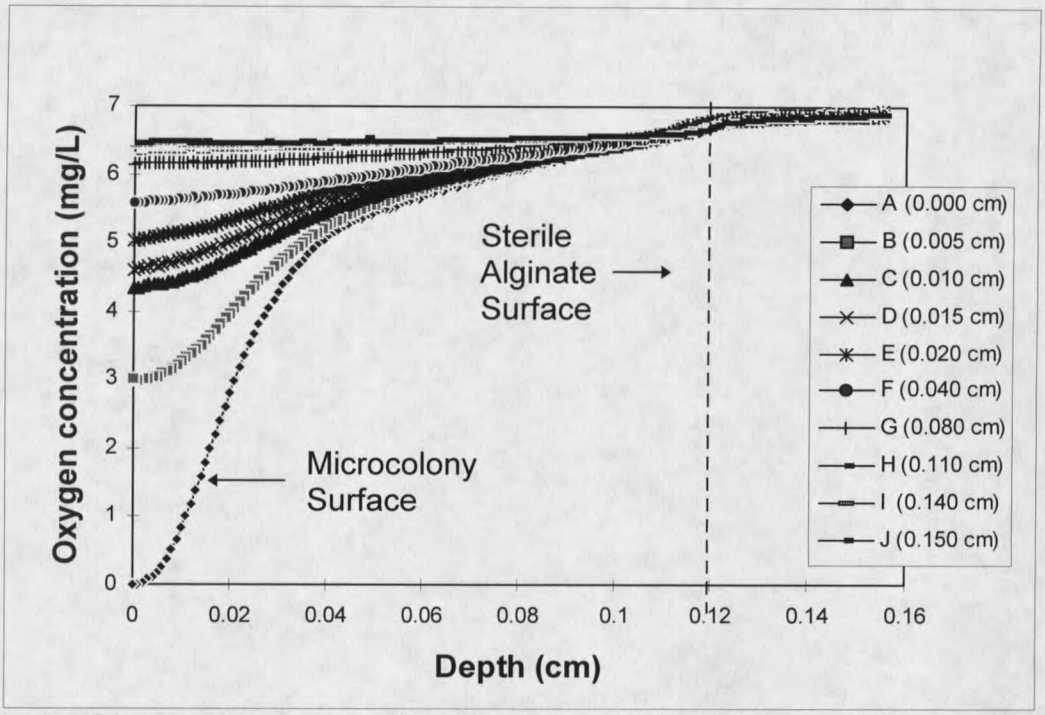


Figure 5. Dissolved oxygen profiles through artificial biofilm containing a single microcolony. Profile (A) was taken directly through the microcolony. Profiles (B-J) were taken at various distances (indicated in the legend) adjacent to the microcolony.

Table 3 shows the diffusivity of oxygen and the microbial respiration kinetics extracted from profile (A) of the heterogeneous artificial biofilm study.

Table 3. Diffusivity and respiration kinetics of heterogeneous biofilm.

Half-Saturation Coefficient (K_S) mg/L	**Maximum Substrate Utilization Rate (V_{Max}) mg/L-sec**	**Diffusivity (D_f) cm^2/sec ---------- % Diffusivity of Water**
0.025	0.44	$2.16(10^{-5})$ 87%

Homogeneous Artificial Biofilm Study

The profiles taken under a low flow velocity (Figures 13-19) and a high flow velocity (Figures 20-26) are presented and analyzed separately in Appendix B. Each profile shows the change in the dissolved oxygen concentration with depth. Figure 6 shows a compilation of all seven profiles (A - G) taken under the low flow velocity conditions (0.04 cm/s), while Figure 7 shows a compilation of all seven profiles (A' - G') taken under the high flow velocity conditions (2.75 cm/s). The flow was in the direction from A to G in both figures. The same biofilm was used under both flow conditions. The biofilm was 1 cm X 2 cm with variable thickness, and had a density of 10^{10} CFU/ mL alginate. The substratum was located at x=0 cm. The insert in Figures 6 and 7 show the approximate shape of the biofilm and locations of the measurements. The biofilm was probed in a linear path down the length of the reactor as indicated in both figures. The length from point B in the reactor to point F was 1 cm. The profiles taken from points B to F were taken near and through the biofilm at approximately 0.25 cm apart. Profiles A and G were taken 0.15 cm upstream and 0.15 cm downstream respectively from the biofilm under both flow velocities.

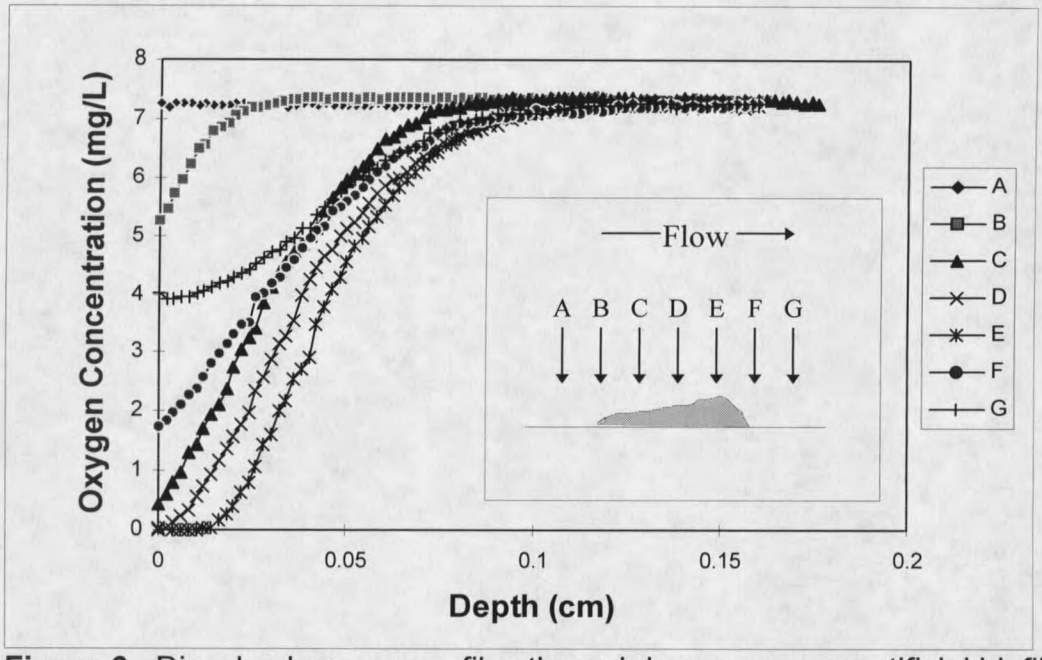


Figure 6. Dissolved oxygen profiles through homogeneous artificial biofilm under low flow velocity. The insert shows the approximate shape of the biofilm and the locations of measurement.

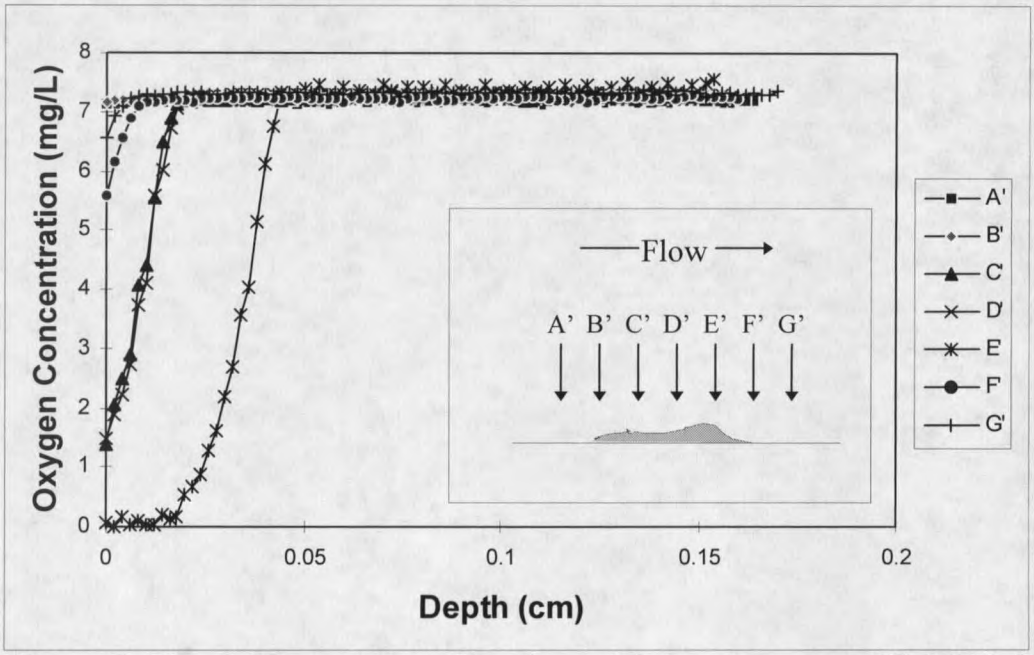


Figure 7. Dissolved oxygen profiles through homogeneous artificial biofilm under a high flow velocity. The insert shows the approximate shape of the biofilm and the locations of measurement.

The substrate diffusivity and microbial respiration kinetics extracted from the profiles taken in the homogeneous artificial biofilm study can be seen in Table 4 (low flow velocity) and Table 5 (high flow velocity).

Table 4. Diffusivity and Respiration Kinetics of the Homogeneous Biofilm-Low Velocity.

	Half-Saturation Coefficient (K_S) mg/L	**Maximum Substrate Utilization Rate (V_{Max}) mg/L-sec**	**Diffusivity (D_f) cm^2/sec ---------- % Diffusivity of Water**
Profile C	U.D.*	-	-
Profile D	U.D.*	-	-
Profile E	0.01	0.09	$1.71(10^{-5})$ 85%
Profile F	U.D.*	-	-

* U.D.- Unable to determine.

Table 5. Diffusivity and Respiration Kinetics of the Homogeneous Biofilm-High Velocity.

	Half-Saturation Coefficient (K_S) mg/L	**Maximum Substrate Utilization Rate (V_{Max}) mg/L-sec**	**Diffusivity (D_f) cm^2/sec ---------- % Diffusivity of Water**
Profile C'	U.D.*	-	-
Profile D'	U.D.*	-	-
Profile E'	0.04	0.27	$1.44(10^{-5})$ 72%

* U.D.- Unable to determine.

Table 6 shows the diffusion boundary layer thickness over the biofilm. The thickness was determined from the profiles taken directly through the biofilm under low and high flow velocities (see Appendix B).

Table 6. Diffusion Boundary Layer Thickness over Biofilm.

Low Flow Velocity	Boundary Layer Thickness (cm)
Profile C	0.04
Profile D	0.052
Profile E	0.046
Profile F	0.052
High Flow Velocity	
Profile C'	0.004
Profile D'	0.004
Profile E'	0.004

Properties of the Artificial Biofilm

Polymer Analysis

The polymer characteristics as characterized by ^{1}H-NMR are given in Table 7.

Table 7. Characteristics of purified alginate from *P. aeruginosa* strain 8830

Property	Native	De-O-acetylated
Molecular Weight (M_W) (g/moles)	$1.8(10^6)$	$1.5(10^6)$
O-acetyl content (moles per uronic acid residue)	0.69	-
Fraction of D-mannuronic acid (F_M)	n.d.	0.95
Fraction of L-guluronic acid (F_G)	n.d.	0.05
Fraction of G units adjacent to a second G (F_{GG})	n.d.	0.00
Fraction of G units adjacent to a M (F_{GM+MG})	n.d.	0.05

n.d.-not determined

Substrate Transport Through Biofilm

Confocal images of the transport study are presented in Figure 8. The white zone in each image is the fluorescein. Image (A) was taken in the bulk fluid of the reactor under stagnant flow conditions. Image (B), taken at the same location as image (A), was under a flow of 3 cm/s. A 'tail' of fluorescein was visible under these conditions in the direction of flow. Image (C) was taken 300 μm below the surface of the alginate layer under stagnant flow conditions. Image (D) was taken in the alginate layer with a flow of 3 cm/s over the alginate.

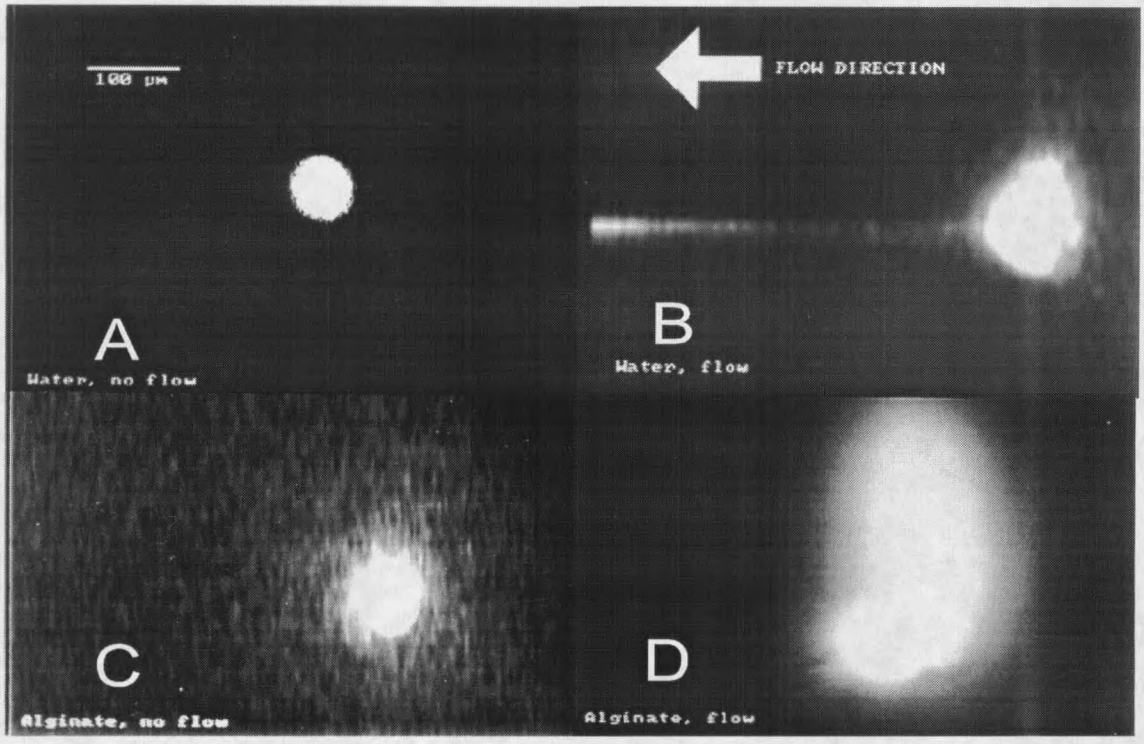


Figure 8. Confocal images of convective transport

Mass Transfer Resistance of the Biofilm Matrix

Bacterial alginate was sterilized using the filter sterilization method described in Chapter 3. No colonies were observed on YTG agar plates inoculated with the filter-treated alginate indicating that the alginate was sterile. As a means of quantifying the mass transport resistance of the biofilm matrix, dissolved oxygen profiles (Figures 9 and 10) were taken through uniform sterile bacterial alginate layers fixed to the reactor surface. The base of the alginate layer is located at x=0 cm. Each figure shows the change in the dissolved oxygen concentration with depth. The average flow velocity over each alginate layer was 2.0 cm/s. The oxygen concentration remained constant throughout the bulk fluid at 7.68 mg/L down to the surface of the alginate. The thickness of the alginate layers were approximately, 0.03 cm for Figure 9, and 0.12 cm for Figure 10. Within the alginate, the oxygen concentration decreased with depth. The percentage decrease in the oxygen concentration from the surface of the alginate to the substratum were, 4.5% for Figure 9, and 5.8% for Figure 10.

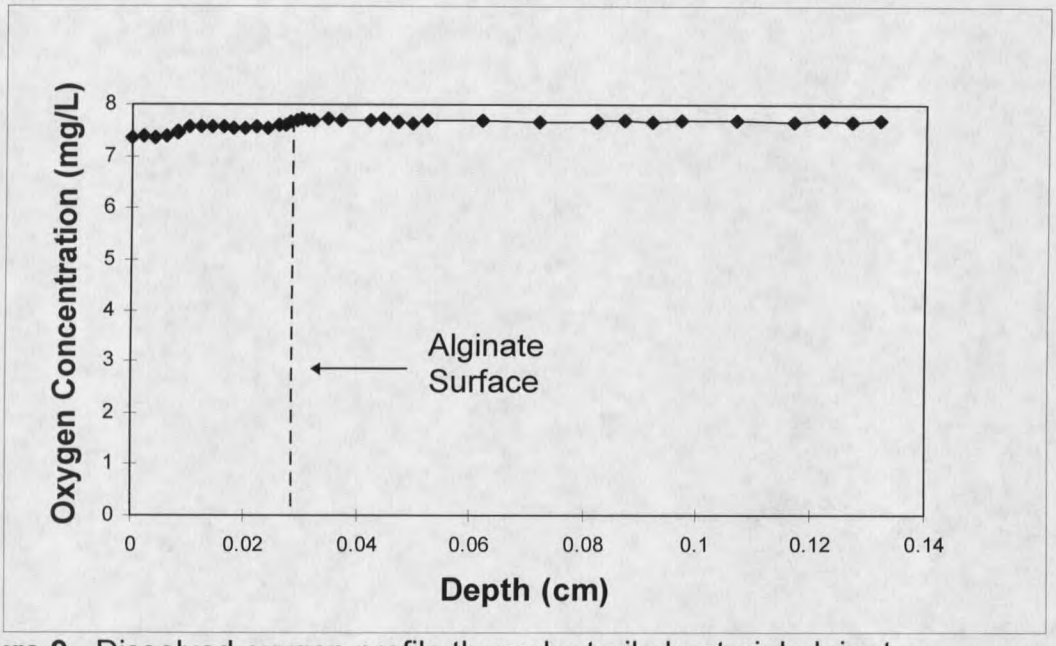


Figure 9. Dissolved oxygen profile through sterile bacterial alginate.

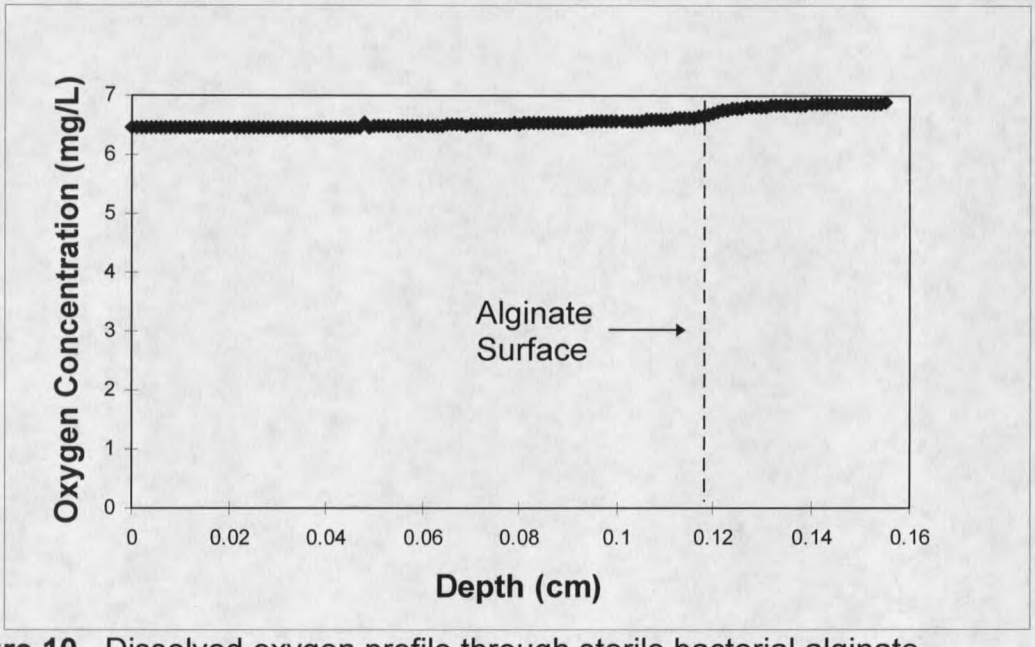


Figure 10. Dissolved oxygen profile through sterile bacterial alginate.

CHAPTER 5

DISCUSSION

Development and Characteristics of the Heterogeneous Artificial Biofilm

A heterogeneous artificial biofilm, which structurally resembled natural biofilm, was developed. This artificial biofilm used bacterial alginate as its polymer matrix instead of the more commonly used kelp alginate. The bacterial alginate, produced by *Pseudomonas aeruginosa* strain 8830, was found to be easily penetrated with microelectrodes. Analysis of the alginate by ^{1}H-NMR (Table 7) showed that the alginate was extensively acetylated with 0.69 moles of O-acetyl groups per mole of uronic acid residues, and that the alginate consisted of 95% mannuronic acid (M) and 5% guluronic acid (G). Of particular importance was the absence of G-blocks, i.e. consecutive sequences of L-guluronic acid. Such G-blocks, found in alginates derived from kelp, are a prerequisite for the formation of firm gels in the presence of calcium ions. This explains why the bacterial alginate studied here did not form a strong gel through the addition of $CaCl_2$ in the nutrient medium and why the bacterial alginate was easily penetrated with microelectrodes.

The alginate was sterilized so the distribution of bacteria could be controlled. A filter sterilization method which preserved the polymers physical integrity similar to that as produced by the bacteria on YTG agar plates was developed. This procedure produced an alginate that was free of bacteria, based on the plating of treated samples onto agar plates as well as direct microscopic observation. Furthermore, this method did not expose the alginate to chemicals or high temperatures which can degrade the alginate changing its physical properties.

The sterilized alginate was then fixed to a substratum where it served as the matrix material of the artificial biofilm. 'Microcolonies' of bacteria, similar to those found in natural biofilms, were formed by microinjection of suspended organisms into localized regions of the biofilm matrix. These 'microcolonies' were on the same scale (<400 μm) as those found in natural biofilm.

Mode of Mass Transport Through Artificial Biofilm

To test the nature of mass transport through the artificial biofilm a dye tracer study was conducted. Using a nanoliter pump, a fluorescein solution, which is fluorescent under a confocal laser microscope, was continuously injected into a sterile bacterial alginate layer fixed to the bottom of an open channel reactor. As shown in image (A) of Figure 8, as the fluorescein was injected into the bulk aqueous water, a uniform sphere formed indicating that transport was occurring equally in all directions. This indicates that under stagnant flow conditions,

transport is governed by diffusion. When flow through the reactor began, the fluorescein plume formed a 'tail' in the direction of flow (image B) due to convective flow. To determine whether convective flow was occurring in the artificial biofilm an identical study was conducted within the alginate layer. However, when fluorescein was released into the alginate layer, a 'tail' did not form on the plume (image D) even when flow (3 cm/s) through the reactor was established. This indicated that convective transport through the alginate was negligible. Thus, using Fick's second law to describe the transport of oxygen in the artificial biofilm appears to be valid.

Mass Transfer Resistance of Biofilm Matrix

The mass transfer resistance of the biofilm matrix can be seen in Figures 9 and 10. These figures show dissolved oxygen profiles taken through sterile alginate layers. Because these profiles were taken in a system free of bacteria, the decrease observed in the profiles immediately upon penetration into the alginate layers was due to the mass transfer resistance exhibited by the polymer matrix. The differences observed in the oxygen concentrations sensed at the alginate surface and at the substratum were ~5%. Thus the mass transfer resistance due to the polymer matrix was considered negligible.

Heterogeneous Biofilm Application

A heterogeneous artificial biofilm was constructed and used to study the effects of a single microcolony on the mass transport of dissolved oxygen. The ten profiles shown in Figure 5 were taken at various horizontal distances from the center of the bacterial drop. Below the alginate-water interface, a decrease in the oxygen concentration was observed in all profiles (A - J). Observation of these profiles indicated that the dissolved oxygen field was affected by the respiratory activity of the bacteria up to a distance of 0.14 cm away from the microcolony. Thus the decrease observed in the profiles (A - I) was due to the consumption of oxygen by the immobilized bacteria and the mass transfer resistance of the polymer gel matrix. However, at a distance greater than 0.040 cm from the microcolony, the decrease in the dissolved oxygen concentration due to its consumption by the microcolony was not as pronounced. Profile (J) was not influenced by the respiring bacteria. The decrease in the oxygen concentration of this profile was solely due to the mass transfer resistance of the alginate matrix and did not appear to be a major barrier to the transport of oxygen.

A final observation of these profiles (A - I) show that in addition to the vertical flux of oxygen into the microcolony, which is equal to the substrate diffusivity coefficient times the concentration gradient (dC/dx), a horizontal flux of oxygen to the microcolony exists as well. This multi-directional flux of oxygen

was a result of only a single microcolony being immobilized which provided a single point of consumption. This flux of oxygen from multiple directions was also responsible for the non-linear shapes of the profiles (A - E) within the biofilm matrix. As seen in profiles (A - E), the slope of the concentration gradient changed at ~0.04 cm above the substratum. This indicates a distinct change in the magnitude of the flux. Isolating profile (A), which was taken directly above and through the microcolony, it can be seen that the relative magnitude of the flux was at its greatest (large dC/dx) from 0.015 to 0.04 cm and decreases in magnitude (smaller dC/dx) from 0.04 to 0.12 cm. The thickness of the zone located just above the microcolony, where the flux was at its greatest, corresponds well with the distance out to profile (E). The non-linearity of profile (E) indicates that at this distance (0.02 cm) from the microcolony, the multi-directional fluxes were large enough in magnitude to alter the shape of this profile. This indicates that the flux of oxygen around the microcolony was in the shape of a hemisphere with its magnitude decreasing further away from the microcolony.

Profile (A), taken directly through the microcolony, was analyzed using the method outlined in Figure 4 to determine the microbial respiration kinetics. Using an oxygen diffusivity through water of 2.5×10^{-5} cm^2/s at 25 °C (Perry, 1984) the parameters, presented in Table 3, were obtained for this biofilm under the conditions previously described. Given the wide range of values reported in literature (Table 2), these values calculated here are reasonable. However, it

should be noted that when applying the procedure outlined in Figure 4 to this data, it broke down in its determination of the half-saturation coefficient (K_S). Only the points lower in the profile behaved linearly as indicated in the procedure outline. A regression of these points resulted in the K_S reported in Table 3. The remainder of the procedure behaved as presented in Figure 4.

Homogeneous Biofilm Study

A homogeneous artificial biofilm was constructed and used to evaluate the procedure which determines the substrate diffusivity and microbial respiration kinetics from substrate concentration profiles. Because the profiles were taken under low (0.04 cm/s) and high flow (2.75 cm/s) velocity conditions, the effects of velocity on the dissolved oxygen profiles were examined as well. Figure 6 shows the seven profiles (A - G) taken under low flow velocity conditions. Figure 7 shows the seven profiles (A' - G') taken under high flow velocity conditions. The profiles in both figures were taken at different points, as indicated in the inserts, down the channel of the reactor. The corresponding profiles from the low and high flow velocity conditions were taken parallel to each other but not at the same locations.

Effects of Flow Velocity on Mass Transport

Profiles A and A' were both taken 0.15 cm upstream from the biofilm. Profile A was taken under the low flow velocity conditions, while profile A' was taken under high flow velocity conditions. Both profiles show that the dissolved oxygen concentration from the bulk fluid to the substratum was constant at 7.24 mg/L . At this point in the reactor there was no alginate layer or biofilm, and thus no consumption or mass transfer resistance of oxygen.

Profiles B and B' were taken at the leading edge of the biofilm. Profile B was taken under the low flow velocity conditions, while profile B' was taken under high flow velocity conditions. In both cases, the microelectrode did not penetrate biofilm at this point in the reactor, but was very close to the leading edge of the biofilm. In profile B, the decrease in the substrate concentration near the substratum was attributed to the probes close proximity to the biofilm. Here, the microelectrode sensed the effects of the respiratory activity of the biofilm on the surrounding dissolved oxygen field, similar to that as seen in Figure 5. In contrast to profile B no decrease in the profile was observed in profile B'. This was due to an increase in the fluid velocity which increased the oxygen transport rate to this point in the reactor. The oxygen was now being replenished faster than it was being consumed by the biofilm.

Profiles C, D, E, F and C', D', E' show the dissolved oxygen concentration gradients taken through the biofilm. Profiles C - F were taken under the low flow velocity conditions, while profiles C' - E' were taken under high flow velocity

conditions. These profiles clearly show the external mass transfer (diffusion) boundary layer which extends from the biofilm surface, into the bulk fluid to a point where the concentration gradient no longer exists. The concentration gradient results from the consumption of oxygen at the biofilm surface. Table 6 shows that the diffusion boundary layer was significantly reduced when the flow velocity was increased from 0.04 cm/s to 2.75 cm/s. The average diffusion boundary layer thickness was 0.048 cm under low flow conditions and 0.004 cm under high flow conditions. This decrease in the thickness of this boundary layer was due to the increase in the flow velocity. When the flow velocity was increased, the hydrodynamic boundary lay decreased as seen in Figure 11. This increased the oxygen transport rate to the biofilm surface which in turn raised the oxygen concentration. Since the flux of oxygen into the biofilm was approximately the same under both conditions, the higher substrate concentration just above the biofilm was maintained, thereby decreasing the thickness of the diffusion boundary layer. The higher substrate concentration above the film also resulted in an increase in the substrate availability to the biofilm as well. The surface oxygen concentration was approximately 4 mg/L under low flow conditions and increased to 6.5 mg/L under high flow conditions. The decrease in the oxygen concentration in the biofilm in each of these profiles was due to its consumption by the bacteria, as well as the mass transfer resistance of the microbial cells, and polymer matrix. These seven profiles were

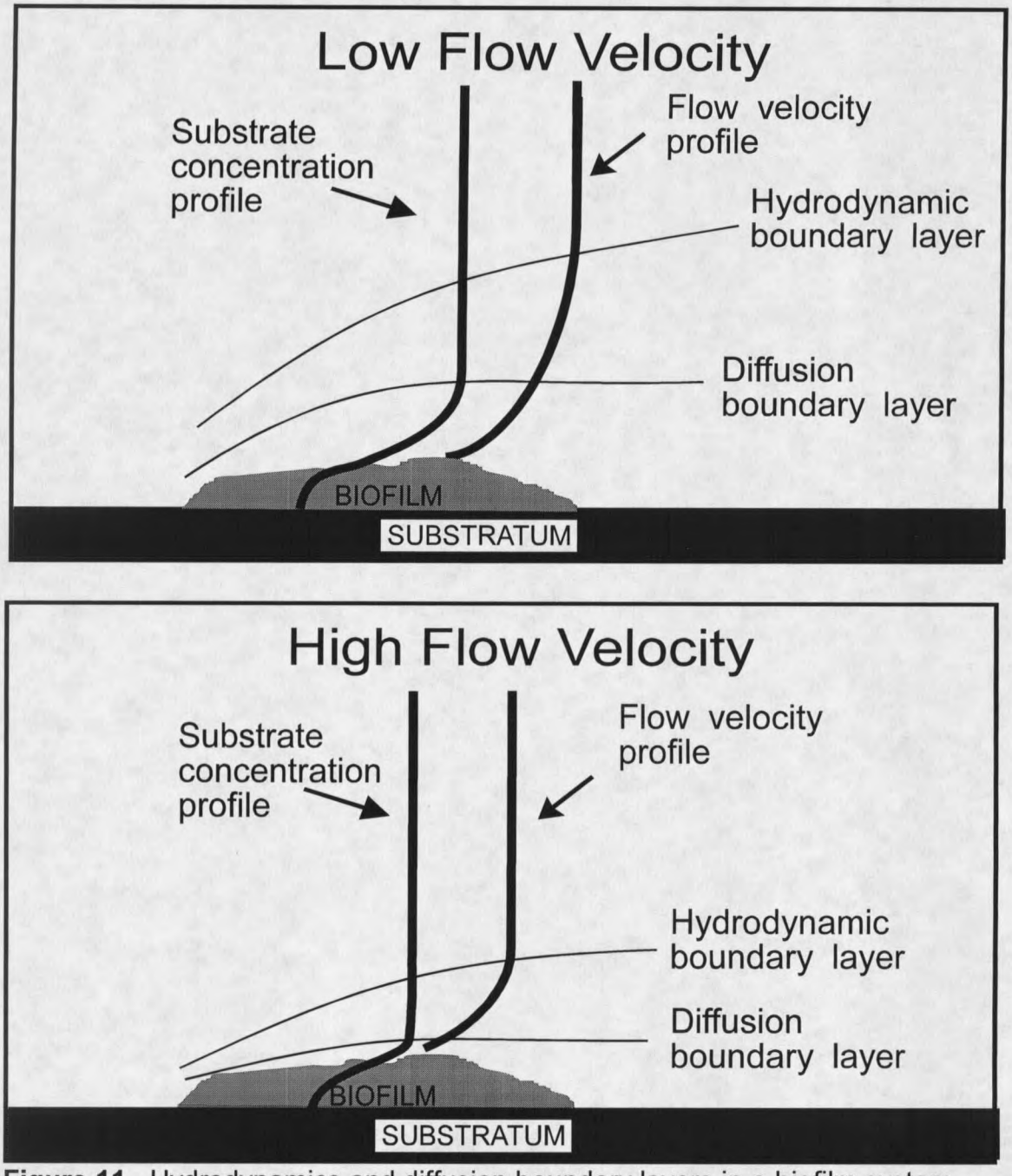


Figure 11. Hydrodynamics and diffusion boundary layers in a biofilm system. The upper figure shows the relative thickness of the hydrodynamic and diffusion boundary layers under a low flow velocity. The lower figure shows the relative thickness of the boundary layers under a high flow velocity (Modified from Lewandowski et al., 1994).

analyzed using the procedure outlined in Figure 4 for the kinetic parameters. Tables 4 and 5 show these results.

Profile F' was taken 1.0 cm from the leading edge of the biofilm under high flow velocity conditions. The microelectrode did not penetrate biofilm at this point in the reactor, but was very close to the edge of the biofilm. The decrease in the profile was attributed to the probes close proximity to the biofilm where it sensed the effects of the respiratory activity of the biofilm on the surrounding dissolved oxygen field, similar to that seen in Figures 5 and profile B.

Profiles G and G' were taken 0.15 cm downstream from the homogeneous biofilm. Profile G was taken under the low flow velocity conditions, while profile G' was taken under high flow velocity conditions. A decrease was observed in the dissolved oxygen concentration in both profiles even though the microelectrode did not penetrate any biofilm at this point in the reactor. The oxygen concentrations at the substratum of these profiles were similar to those observed at the surface of the biofilm. Therefore, the decrease observed in both profiles was attributed to the depletion of oxygen by the biofilm located upstream. As the water flows downstream, at this point in the reactor, not enough time has elapsed to allow the depleted substrate concentration to be replenished with oxygen from the bulk fluid.

Oxygen Diffusivity and Microbial Respiration Kinetic Analysis

Several profiles (C - F and C' - E') were generated through a homogeneous artificial biofilm for evaluation of the procedure used to extract the microbial respiration kinetics from substrate concentration profiles. This procedure was evaluated for its applicability and reproducibility in analyzing the profiles taken in the artificial biofilm system. If this procedure can be used to analyze data from the artificial biofilm, the diffusivities and kinetic parameters (V_{Max} and K_S) calculated from these profiles should be similar, irregardless of alterations in the flow velocity. The protocol of this procedure (Figure 4) was adhered to closely using third and fourth order polynomials to describe the data.

The applicability of this procedure to analyzing profiles taken in the artificial biofilm system was evaluated. Tables 4 and 5 show the respiration kinetics parameters analyzed from the dissolved oxygen concentration profiles. These tables show that several profiles (C, D, F, C' and D') were unable to be analyzed using the procedure outlined in Figure 4. These profiles were all taken at points in the biofilm which were fully-penetrated with respect to the limiting substrate oxygen. When analyzing the data from these profiles, deviations from the expected trends were seen. In contrast profiles E and E', which were partially-penetrated with respect to oxygen could be analyzed using the procedure in Figure 4 producing reasonable kinetic values. Because the degree of substrate penetration greatly influences the shape of the profiles it became

apparent that the shape of the profile was the governing factor as to whether or not this procedure could be used to analyze the concentration profiles.

The procedures ability to generate reproducible results was evaluated. Profile E and E' were the only profiles which could be analyzed using the technique outlined in Figure 4. As seen in Tables 3, 4 and 5 the values obtained for the half-saturation coefficient (K_S) were very similar. Because the same organism *P. aeruginosa* strain 8830 was used in all studies, K_S an intrinsic kinetic parameter, should not change due to alterations of the flow velocity over the biofilm, or from point to point in the biofilm. It should be noted that when applying this procedure to determine the value of K_S, only the data points at the lower concentrations on the profiles behaved in a linear fashion and could thus be used to determine K_S. A regression was made on these points and K_S was determined. It is hypothesized that because the K_S for oxygen is so small (<0.5 mg/L), the concentration of oxygen higher in the biofilm can not be used to determine its value. This is why only the points lower in the biofilm, which are closer in magnitude to the K_S value, behave in a linear fashion. The slight variations seen in the magnitude of K_S were probably due to "electrical noise" (random increase and decreases in the data points, not related to oxygen concentration) in the profiles. Because so few (4-5) data points were used to determine K_S any "noise" in these points would alter the slope of the regression thus affecting the K_S value.

Values obtained for the maximum substrate utilization rate (V_{Max}) will be constant throughout the biofilm if and only if the biomass does not change over time or from point to point in the biofilm. This is because V_{Max} in microbial kinetics as defined in equation (3) is not independent of biomass concentration. Therefore, the differences observed in this study may have been due to one or more of the following reasons. First, it is possible that the microorganisms were growing in the artificial biofilm and therefore the biomass concentration was changing. This increase may not be significant between two profiles taken consecutively, but could be between profiles taken several hours apart as profiles E and E' were. Secondly, if the assumption of uniformly distributed bacteria was not correct, the biomass concentration would have changed from point to point in the biofilm resulting in a change of V_{Max}. Since a substrate concentration profile taken through the biofilm with a microelectrode is representative of only one point within the biofilm, the information extracted from this profile can only accurately describe the biofilm activity at that point. Therefore, when a value for V_{Max} is obtained from the profile, it is only valid for that point in the biofilm, under those conditions, including the biomass concentration. Finally, changes in V_{Max} may have arisen from the influences of local hydrodynamics on the shape of the concentration profiles. As seen in Figures 6 and 7 alterations in the flow velocity had a direct effect on the concentration of dissolved oxygen at the biofilm surface. Under a high flow velocity more oxygen was now available for diffusion through the biofilm surface.

If consumption remained constant, this would result in an increase in the substrate concentration higher in the biofilm which would alter the shape of the profile. Since the shape of the profile will determine the values obtained for the kinetic parameters, V_{Max} could still experience changes even though the bacterial concentration and distribution were constant as assumed.

Finally, the problems encountered with this procedure may have been due to the many assumptions which were made when applying this model (equation 5) to the data. The assumptions were: 1) cell density was uniform throughout the biofilm in space and time, 2) oxygen was the only limiting nutrient, 3) transport through the biofilm follows Fick's second law, 4) molecular diffusivity of oxygen was constant in the biofilm, 5) the system was considered to be at steady state, and 6) oxygen uptake followed Monod kinetics. A breakdown in any of these assumptions may cause the model used in the outlined procedure to be invalid. The difficulty of checking the validity of these assumptions is that they are usually made because it is not possible, or is difficult to determine that property or behavior independently.

Given the wide range of values reported in literature (Table 2) the values calculated and presented in Tables 4 and 5 are reasonable. Although theoretically sound, the procedure as previously mentioned, proved to be difficult to apply to some data taken in the artificial biofilm. Given these problems, and thus the low number of profiles that were capable of being analyzed, it is difficult

to make any conclusive statements as to whether or not changes in the velocity had any effect on the kinetics.

Possible Limitations of the Artificial Biofilm

The heterogeneous artificial biofilm can not entirely replace studies involving natural biofilm. This is in part due to limitations with its use. The following areas have been identified as being possible limitations with use of the artificial biofilms developed in this research.

- To date, the artificial biofilm has only been used on glass surfaces. Other materials which may serve as a substratum have not been tried except for mild steel which had limited success. On mild steel the biofilm would "slough-off" after only a short time in the reactor.
- The requirement of the specially designed medium may restrict the microorganisms which can be used. Theoretically, any organism which can be grown in batch or chemostat cultures can be immobilized in the artificial biofilm. However, this medium was developed as a growth medium for the organism *Pseudomonas aeruginosa* strain 8830 and was not tested on other organisms. It is recommended that any microorganism, which is considered for use in the artificial biofilm, be cultured on this medium in a batch or chemostat reactor to ensure that the medium satisfies the growth requirements of that organism.

- With the current method of immobilization, it is difficult to inject several microcolonies quickly into a thin layer of alginate before dehydration of the polymer layer occurs. This may limit studies involving this type of biofilm to simple structures (i.e. containing few microcolonies).

Advantages and Applications of Artificial Biofilms

The biofilms developed in this work (heterogeneous structure) contained several improvements over the commonly used homogeneous artificial biofilms. First, the biofilm developed in this work did not use kelp alginate or agar, the two most commonly used polymers for artificial biofilms. This artificial biofilm was composed of bacterial alginate, a polymer that can be found in some natural biofilms. Instead of a uniform distribution of bacteria throughout the polymer matrix, this biofilm contained bacterial aggregations (microcolonies). These 'microcolonies' were made on the same scale as those found in natural biofilm, making it possible to produce artificial biofilms which are on the same scale as natural biofilms. This biofilm was also fixed to a substratum conforming to the definition of biofilm. Finally, this artificial biofilm can be easily penetrated with microelectrodes allowing concentration gradient (i.e. substrate, pH, ions, etc.) to be easily measured through the biofilm.

Artificial biofilm are useful laboratory tools allowing some experiments to be carried out in a more controlled and reproducible environment. These

synthetic biofilms are easy to assemble, have well defined physical parameters and can produce results quickly. Unlike natural biofilms, through the use of a heterogeneous artificial biofilms, many physical and experimental parameters including bacterial distribution, bacterial density and biofilm thickness can be fixed allowing each experiment to be run under the same conditions. Use of this artificial biofilm will enable studies involving biofilm to be conducted under conditions more similar to those experienced in natural biofilm studies. This will enable data to be produced which more closely resembles the behavior of a natural biofilm system.

These synthetic biofilms can be constructed and used anywhere that a biofilm with a well defined geometry and known biofilm activity are needed. More specifically, areas of research involving mass transport, biocide/antibiotic efficacy testing, and model validation will benefit from the use of artificial biofilms.

CHAPTER 6

CONCLUSIONS

1) A heterogeneous artificial biofilm has been developed. This biofilm used bacterial alginate as its polymer matrix material, incorporated 'microcolonies' of bacteria as seen in natural biofilm, and was easily penetrated with microelectrodes.

2) The predominant mode of transport through the artificial biofilm matrix was by molecular diffusion. This makes Fick's second law a valid choice for use in the reaction-diffusion model.

3) A study involving the heterogeneous artificial biofilm, demonstrated the applicability of this type of biofilm for monitoring the effects of biofilm heterogeneity on mass transport. This study indicated that the surrounding dissolved oxygen field was affected by a single microcolony (150 μm diameter, 10^{10} CFU/ mL alginate) up to 1400 μm from the microcolony and that the mass transfer resistance of the biofilm matrix was negligible.

4) A study involving a homogeneous artificial biofilm indicated that the procedure used for extracting microbial respiration kinetics from substrate concentration profiles had problems for use in analyzing profiles taken in the

artificial biofilm which were fully-penetrated with respect to oxygen. Partially-penetrated oxygen profiles could be analyzed with this procedure and produced kinetic parameters which were reasonable in comparison to values found in literature. In addition the values obtained for K_S, an intrinsic kinetic parameter, were very similar amongst the three conditions probed (single microcolony, and two flow velocities) showing good reproducibility in analyzing the data. The visual analysis of the profiles generated through this biofilm under the low and high flow velocity conditions, showed that the diffusion boundary layer was significantly influenced by flow velocity. This boundary layer decreased from 0.048 cm to 0.004 cm when the flow velocity was changed from low (0.04cm/s) to high (2.75 cm/s). A direct result of this decrease, was a higher substrate concentration at the biofilm surface. The surface concentration was approximately 4 mg/L under low flow conditions and increased to 6.5 mg/L under high flow conditions. This increased the substrate availability to the biofilm.

5) These mass transport studies are one example of how artificial biofilms are useful laboratory tools which allow some experiments involving biofilms to be carried out in a more controlled and reproducible environment. Several other applications exist as artificial biofilms can be used wherever there is a need for a biofilm with a well defined geometry and bacterial activity.

Nomenclature

[Units:M--mass, L--length, T--time]

A is an experimental coefficient.

C is the concentration of substrate, (ML^{-3}).

C_b is the concentration of substrate in the bulk fluid, (ML^{-3}).

C_O is the concentration of substrate at the substratum, (ML^{-3}).

C_S is the concentration of substrate at the biofilm surface, (ML^{-3}).

D_e is the diffusion coefficient of the substrate, (L^2T^{-1}).

K_S is the half saturation coefficient, (ML^{-3}).

Re is the Reynolds number, ($=V*R_h/\nu$).

R_h is the hydraulic radius, (L).

t is the time, (T).

μ_{Max} is the maximum growth rate, (T^{-1}).

ν is the kinematic viscosity, (L^2T^{-1}).

V is the average flow velocity, (LT^{-1}).

V_{Max} is the maximum substrate utilization rate, ($ML^{-3}\ T^{-1}$).

x is the distance from substratum, (L).

x_S is the biofilm thickness, (L).

X is the biomass concentration, (ML^{-3}).

$Y_{X/S}$ is the biomass yield , (ML^{-3} biomass/ML^{-3} substrate).

REFERENCES CITED

Alexander, M., and Scow, K.M. (1989) Kinetics of biodegradation in soil. In Reactions and Movement of Organic Chemicals in Soils. pp. 243-268, Soil Science Society of America and American Society of Agronomy, Madison, WI.

Bergey, D.H, Krieg, N.R., Holt, J.G. (eds) (1984) Bergey's manual of systematic bacteriology. Vol. 1. pp.140-142. Williams & Wilkins, Baltimore, MD.

Brown, M.J., and Lester, J. N. (1980) Comparison of bacterial extracellular polymer extraction methods. Appl. Environ. Microbiol. **40**, 179-185.

Bungay, H.R., Whalen W.J., and Sanders W.M. (1969) Microprobe techniques for determining diffusivities and respiration rates in microbial slime systems. Biotechnol. Bioeng. **11**, 765-772.

Chang, H.N., and Moo-Young, M. (1988) Estimation of oxygen penetration depth in immobilized cells. Appl. Microbiol. Biotechnol. **29**, 107-112.

Characklis, W.G., and Cooksey, K.E. (1983) Biofilms and microbial fouling. Adv. Appl. Microbiol. **29**, 93-132.

Characklis, W.G., McFeters, G.A., and Marshall, K.C. (1990) Physiological ecology in biofilm systems. In Biofilms (Characklis, W.G., and Marshall, K.C. eds) pp.366, 740. John Wiley & Sons. New York.

Chen, K., and Huang, C. (1988) Effects of the growth of *Trichosporon cutaneum* in calcium alginate gel beads upon bead structure and oxygen transfer characteristics. Enzyme Microb. Technol. **10**, 284-291.

Chen, Y.S., and Bungay, H.R. (1981) Microelectrode studies of oxygen transfer in trickling filter slimes. Biotechnol. Bioeng. **23**, 781-792.

Costerton, J.W. (1994) Structure of biofilms. In Biofouling and Biocorrosion in Industrial Water Systems. (Geesey, G.G., Lewandowski, Z., and Flemming, H.C. eds.), pp. 1-14 Lewis Publishers Inc., Chelsea MI.

Cottrell, I.W., and Kovacs, P. (1977) Algin. In Food Colloids. (Graham, H.D., eds.) pp. 439-459. The AVI Publishing Company, Westport, CT.

Darzins, A., and Chakrabarty, A.M. (1984) Cloning of genes controlling alginate biosynthesis from a mucoid cystic fibrosis isolate of *Pseudomonas aeruginosa*. J. Bacteriol. **159**, 9-18.

Fan, L.S., Leyva-Ramos, R., Wisecarver, K.D., and Zehner, B.J. (1990) Diffusion of phenol through a biofilm grown on activated carbon particles in a draft-tube thress-phase fluidized-bed bioreactor. Biotechnol. Bioeng. **35**, 279-286.

Gacesa, P., and Russell, N.J. (1990) The structure and properties of alginate. In Pseudomonas Infection and Alginates, Biochemistry, Genetics and Pathology, pp. 29-49, Chapman and Hall.

Grasdalen, H. (1983) High-field 1-H-n.m.r. spectroscopy of alginate: Sequential structure and linkage conformations. Carbohydr. Res. **118**, 255-260.

Hannoun, B., and Stephanopoulos, G. (1986) Diffusion coefficients of glucose and ethanol in cell-free and cell-occupied calcium alginate membranes. Biotechnol. Bioeng. **28**, 829-835.

Harremoës, P. (1978) Biofilm Kinetics. In Water Pollution Microbiology (Edited by Mitchell R.), pp. 77-110. Wiley, New York.

Hiemstra, H., Dijkhuizen, L., and Harder, W. (1983) Diffusion of oxygen in alginate gels related to the kinetics of methanol oxidation by immobilized *Hansenula polymorpha* cells. Eur. J. Appl. Microbiol. Biotechnol. **18**,189-195.

Hooijmans, C.M., Geraats, S.G.M., and Luyben, K. (1990a) Use of an oxygen microsensor for the determination of intric kinetic parameters of an immobilized oxygen reducing enzyme. Biotechnol. Bioeng. **35**, 1078-1087.

Hooijmans, C.M., Ras, C., andLuyben, K. (1990b) Determination of oxygen profiles in biocatalyst particles by means of a combined polarographic oxygen microsensor. Enzyme Microb. Technol. **12**, 178-183.

Hooijmans, C.M., Geraats, S.G.M., van Neil, E.W.J., Robertson, L.A., Heijnen, J.J., and Luyben, K. (1990c) Determination of growth and coupled nitrification/denitrification by immobilized *Thiosphaera pantotropha* using measurement and modeling of oxygen profiles. Biotechnol. Bioeng. **36**: 931-939.

Hulst, A.C., Hens, H.J.H., Buitelaar, R.M., and Tramper, J. (1989) Determination of the effective diffusion coefficient of oxygen in gel materials in relation to gel concentration, Biotechnol. Tech. **3**, 199-204.

Iribarne, A.P.D., Marchiano, S.L., and Arvia, A.J. 1970. Ionic mass transfer in channel electrodes under laminar flow. Electrochim. Acta. **15**,1827-1836.

Jørgensen, B.B., and Revsbech, N.P. (1988) Microsensors. In Methods in Enzymology. (Packer, L., and Glazer, A.N. eds.), **167**, 639-659, Academic Press Inc., San Diego CA.

Jouenne, T., Tresse, O., and Junter, G. (1994) Agar-entrapped bacteria as an in vitro model of biofilms and their susceptibility to antibiotics. FEMS Microbiol. Lett. **119**, 237-242.

Kuhn, R., Peretti, S., and Ollis, D. (1991) Microfluorimetric analysis of spatial and temporal patterns of immobilized cell growth. Biotechnol. Bioeng. **38**, 340-352.

Kurosawa, H., Matsumura, M., and Tanaka, H. (1989) Oxygen diffusivity in gel beads containing viable cells. Biotechnol. Bioeng. **34**, 926-932.

Larsen, T., and Harremoës, P. (1994) Combined reactor and microelectrode measurements in laboratory grown biofilms. Water Res. **28**, 1435-1441.

Lewandowski, Z., Walser, G., and Characklis, W.G. (1991) Reaction kinetics in biofilms. Biotechnol. Bioeng. **38**, 877-882.

Lewandowski,Z., Altobelli, S., and Fukushima, E. (1993) NMR and microelectrode studies of hydrodynamics and kinetics in biofilms, Biotechnol. Prog. **9**,40-45.

Lewandowski, Z. (1994) Dissolved oxygen gradients near microbially colonized surfaces. In Biofouling and Biocorrosion in Industrial Water Systems. (Geesey, G.G., Lewandowski, Z., and Flemming, H.C. eds.), pp.175-188, Lewis Publishers Inc., Chelsea MI.

Lewandowski, Z., Stoodley, P., Altobelli, S., and Fukushima, E. (1994) Hydrodynamics and kinetics in biofilm systems - recent advances and new problems. Wat. Sci. Tech. **29**, 223-229.

Linker, A., and Jones, R. (1966) A new polysaccharide resembling alginic acid isolated from pseudomonads. J. Biol. Chem. **241**, 3845-3851.

Martinsen, A., Skjåk-Bræk, G., and Smidsrød, O. (1989) Alginate as immobilization material: I. correlation between chemical and physical properties of alginate gel beads. Biotechnol. Bioeng. **33**: 79-89.

Martinsen, A., Storrø, I., and Skjåk-Bræk, G. (1992) Alginate as immobilization material: iii. diffusional properties, Biotechnol. Bioeng. **39**, 186-194.

Matson, J.V., and Characklis, W.G.(1976) Diffusion into microbial aggregates. Water Res. **10**,877-885.

Mattila-Sandholm, T., and Wirtanen, G. (1992) Biofilm formation in the Industry: a review. Food Reviews Internation. **8**, 573-603.

Matulovic, U., Rasch, D., and Wagner, F. (1986) New equipment for the scaled up production of small spherical biocatalysts. Biotechnol. Lett. **8**, 485-490.

Monod, J. (1949) The growth of bacterial cultures. Ann. Rev. Microbiol. **3**, 371-393.

Muslu, Y. (1993) Mass transfer and substrate utilizaiton in biofilm reactors, J. Chem. Tech. Biotechnol. **57**, 127-135.

Ogbonna, J., Matsumura, M., and Kataoka, H. (1991) Effective oxygenation of immobilized cells through reduction in bead diameters: a review, Proc. Biochem. **26**,109-121.

Onuma, M., Onuma, T., Umita, T., and Aizawa, J. (1985) Diffusion coefficient and its dependecy on some biochemical factors. Biotechnol. Bioeng. **27**, 1533-1539.

Patel, T.D., and Bott, T.R. (1991) Oxygen diffusion through a developing biofilm of *Pseudomonas flourescens*. J. Chem. Tech. Biotechnol. **52**, 187-199.

Perry, R.H., and Green D.W. eds. (1984) Perry's Chemical Engineers' Handbook 6th edition , McGraw-Hill Inc.

Revsvech, N., and Ward, D. (1983) Oxygen microelectrode that is insensitive to medium chemical composition: use in an acid microbial mat dominated by *Cyanidium caldarium.* Appl. Environ. Microbiol. **45**, 755-759.

Revsbech, N.P., Madsen, B., and Jørgensen, B.B. (1986) Oxygen production and consumption in sediments determined at high spatial resolution by computer simulation of oxygen microelectrode data. Limnol. Oceanogr. **31**, 293-304.

Revsbech, N.P. (1989) Diffusion characteristics of microbial communities determined by use of oxygen microsensors. J. Microbiol. Meth. **9**, 111-122.

Rittman, B.E., and McCarty, P.L. (1980) Model of steady-state biofilm kinetics. Biotechnol. Bioeng. **22**, 2343-2357.

Rittman, B.E., Crawford, L., Tuck,C.K., and Namkung, E. (1986) *In situ* determination of kinetic parameters for biofims: isolation and characterization of oligontrophic biofilms. Biotechnol. Bioeng. **28**, 1753-1760.

Rudd, T., Sterritt, R. M., and Lester J. N. (1984) Formation and conditional stability constants of complexes formed between heavy metals and bacterial extracellular polymers. Water Res. **18**, 379-384.

Ruiz-Bevia, F., Fernandez-Sempere, J., Colom-Valiente, J. (1989) Diffusivity measurement in calcium alginate gel by holographic interferometry. AIChE Journal. **35**, 1895-1898.

Sanders III, W.M., Bungay III, H.R. and Whalen, W.J. (1970) Oxygen microprobe studies on microbial slime films. Water. **67**, 69-74.

Sato, K., and Toda, K. (1983) Oxygen uptake rate of immobilized growing *Candida lipolytica*. J. Ferment. Technol. **61**, 239-245.

Shuler, M., and Kargi, F. (1992) How cells grow. In Bioprocess Engineering, Basic Cencepts, p. 170. Prentice Hall, Englewood Cliffs, New Jersey.

Siegrist, H., and Gurjer, W. (1985) Mass transfer mechanisms in a heterotrophic biofilm. Water Res. **19**, 1369-1378.

Skjåk-Bræk, G., Grasdalen, H., and Smidsrød, O. (1989a) Inhomogeneous polysaccharide ionic gels. Carbohydr. Polym. **10**, 31-54.

Skjåk-Bræk, G., Zanetti, G F., and Paoletti, S., (1989b) Effect of acetylation on some solution and gelling properities of alginates. Carbohydr. Res. **185**, 131-138.

Smidsrød, O. (1970) Solution properties of alginate. Carbohyd. Res. **13**, 359-372.

Smidsrød, O., and Haug, A. (1972) Properities of poly(1,4-hexuronates) in the gel state. Acta Chem. Scand. **26**, 79-88.

Smidsrød, O. (1974) Molecular basis for some physical properties of alginates in the gel state. Faraday Discussions of the Amer. Chem. Soc. **57**,263-274.

Smidsrød, O., and Skjåk-Bræk G. (1990) Alginate as immobilization matrix for cells. Tibtech. **8**, 71-78.

Stoodley, P., DeBeer, D., Lewandowski, Z. (1994) Liquid flow in biofilm systems. Appl. Environ. Microbiol. **60**, 2711-2716.

Stormo, K., and Crawford, R. (1992) Preparation of encapsulated microbial cells for environmental applications. Appl. Environ. Microbiol. **58**, 727-730.

Sun, Y. Furusaki, S., Yamauchi, A., and Ichimura, K. (1989) Diffusivity of oxygen into carriers entrapping whole cells. Biotechnol. Bioeng. **34**, 55-58.

Tang W.T., and Fan L.S. (1987) Steady state phenol degradation in a draft-tube, gas-liquid-solid fluized-bed bioreactor. AIChE Journal. **33**, 239-249.

Toth, D., Tomasovicova, D., Gemeiner, P., and Kurillova, L. (1988) Metabolic characteristics of bacterial cells entrapped in beaded calcium alginate and/or pectate gels. **34**, 515-524.

Whitham, T.S., and Gilbert, P.D. (1993) Evaluation of a model biofilm for the ranking of biocide performance against sulphate-reducing bacteria. J. Appl. Bacteriol. **75**, 529-535.

Wiseman, A. (ed.) (1983) Enzymology and biotechnology. In Principles of Biotechnology, p. 147. Surrey University Press, New York.

Woodward, J. (1988) Methods of immobilization of microbial cells. J. Microbiol. Meth., **8**, 91-102.

APPENDICES

Appendix A

Microelectrode Reproducibility

The reproducibility of the microelectrode was shown in Figure 12. This figure shows two dissolved oxygen profiles taken at approximately the same location near the edge of the microcolony within the heterogeneous artificial biofilm. The microcolony had a 0.015 cm diameter with a density of 10^{10} CFU/ mL alginate. The base of the biofilm was located at x=0 cm. The average flow velocity over the biofilm was 2.0 cm/s. The alginate-water interface was located at 0.12 cm. The dissolved oxygen concentration above this interface was constant throughout the bulk fluid at 6.8 mg/L. Below this interface a decrease in the oxygen concentration was observed in the two profiles. The profiles show similar trends, indicating good reproducibility of the microelectrode. However, these profiles did deviate slightly from one another. Because these profiles were not taken in exactly the same locations the probe may have encountered different physical parameters of the biofilm (i.e. changes in polymer density) which altered the dissolved oxygen levels in the biofilm.

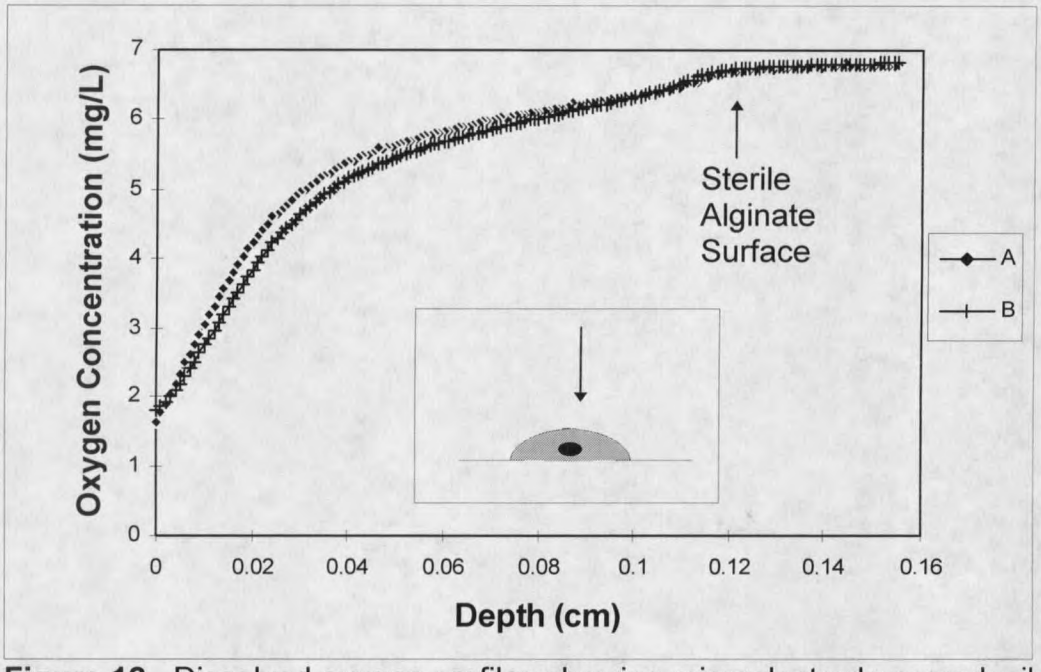


Figure 12. Dissolved oxygen profiles showing microelectrode reproducibility. These profiles were taken at approximately the same location in the artificial biofilm along the edge of the microcolony.

Appendix B

Dissolved Oxygen Profiles Through Homogeneous Artificial Biofilm

Low Flow Velocity

Figure 13 shows the dissolved oxygen profile (A) taken 0.15 cm upstream from the biofilm. The profile maintained a value of 7.24 mg/L throughout the entire depth.

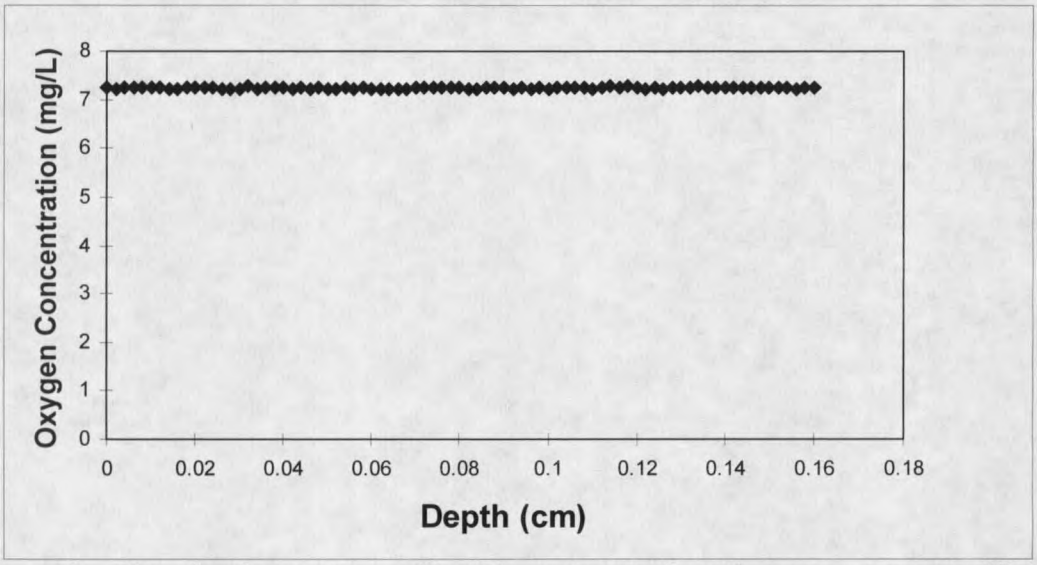


Figure 13. Dissolved oxygen profile (A) upstream from homogeneous artificial under a low flow velocity.

Figure 14 shows profile (B) which was taken at the leading edge of the biofilm. The microelectrode measured a constant oxygen value of 7.24 mg/L down to the point approximately 0.02 cm from the substratum. At this point the dissolved oxygen concentration began to decrease to a concentration of 5.2 mg/L at the substratum.

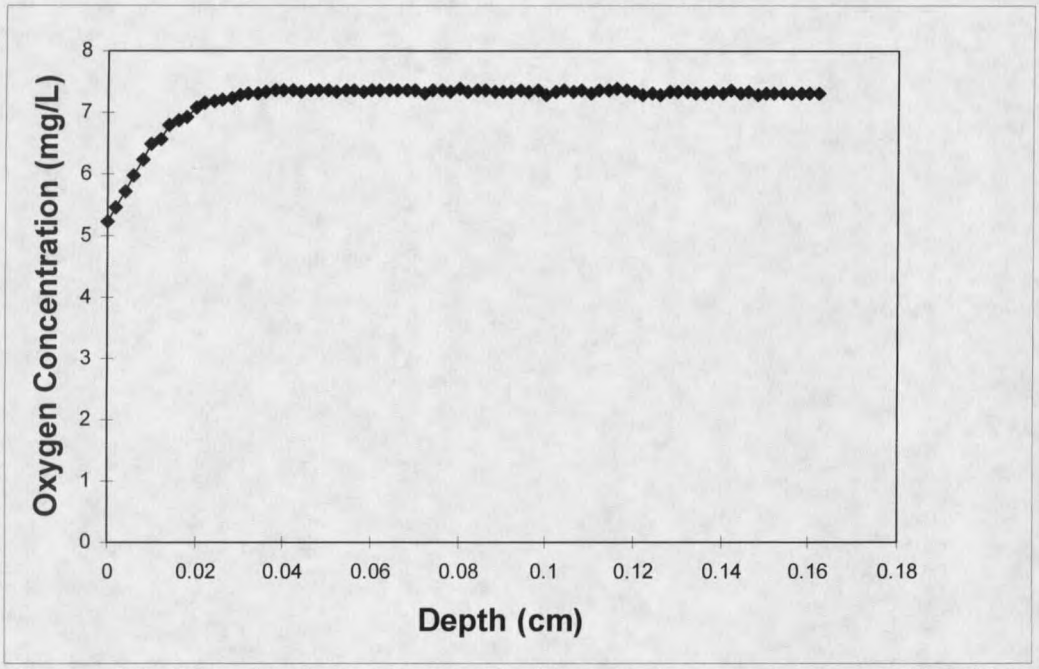


Figure 14. Dissolved oxygen profile (B) near homogeneous artificial biofilm under a low flow velocity.

Figure 15 shows the dissolved oxygen profile (C) taken 0.25 cm from the leading edge of the biofilm (point B on figure 6). The thickness of the biofilm at this point was 0.028 cm. Above x=0.08 cm the profile shows a constant oxygen value of 7.24 mg/L in the bulk fluid. From 0.028 cm to 0.068 the mass transfer boundary layer that exists between the bulk fluid and biofilm can be seen. This external mass boundary layer was 0.04 cm thick. From x=0 cm to x= 0.028 cm is the portion of the dissolved oxygen profile taken inside the biofilm. The biofilm at this location was fully penetrated with a concentration of 0.5 mg/L at the substratum.

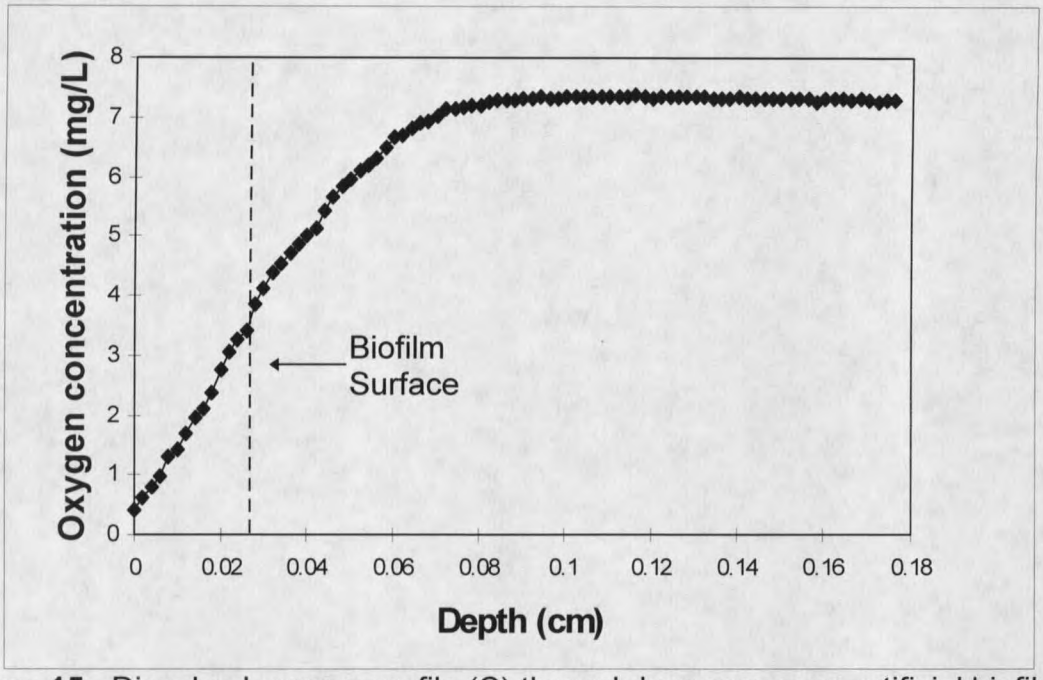


Figure 15. Dissolved oxygen profile (C) through homogeneous artificial biofilm under a low flow velocity.

Figure 16 shows the dissolved oxygen profile (D) taken 0.5 cm from the leading edge of the biofilm. The thickness of the biofilm at this point was 0.038 cm. Above x=0.10 cm the profile shows a constant oxygen value of 7.24 mg/L in the bulk fluid. From 0.038 cm to 0.09 the mass transfer boundary layer that exists between the bulk fluid and biofilm can be seen. This external mass boundary layer was 0.052 cm thick. From x=0 cm to x= 0.038 cm is the portion of the dissolved oxygen profile taken inside the biofilm. The biofilm at this location was almost fully penetrated, and had an oxygen concentration of 0.0 mg/L at the substratum.

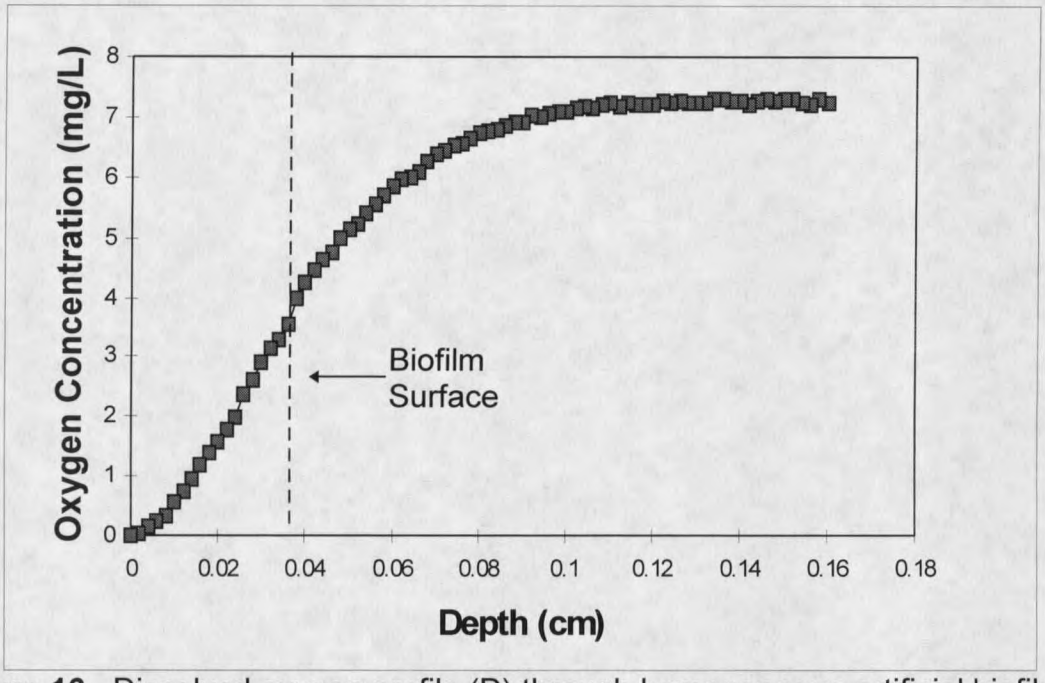


Figure 16. Dissolved oxygen profile (D) through homogeneous artificial biofilm under a low flow velocity.

Figure 17 shows the dissolved oxygen profile (E) taken 0.75 cm from the leading edge of the biofilm. The thickness of the biofilm at this point was 0.042 cm. Above x=0.10 cm the profile shows a constant oxygen value of 7.24 mg/L in the bulk fluid. From 0.042 cm to 0.088 the mass transfer boundary layer above the biofilm can be seen. This external mass boundary layer was 0.046 cm thick. From x=0 cm to x= 0.042 cm is the portion of the dissolved oxygen profile taken inside the biofilm. The biofilm at this location was partially penetrated with oxygen concentration going to 0.0 mg/L at 0.012 cm.

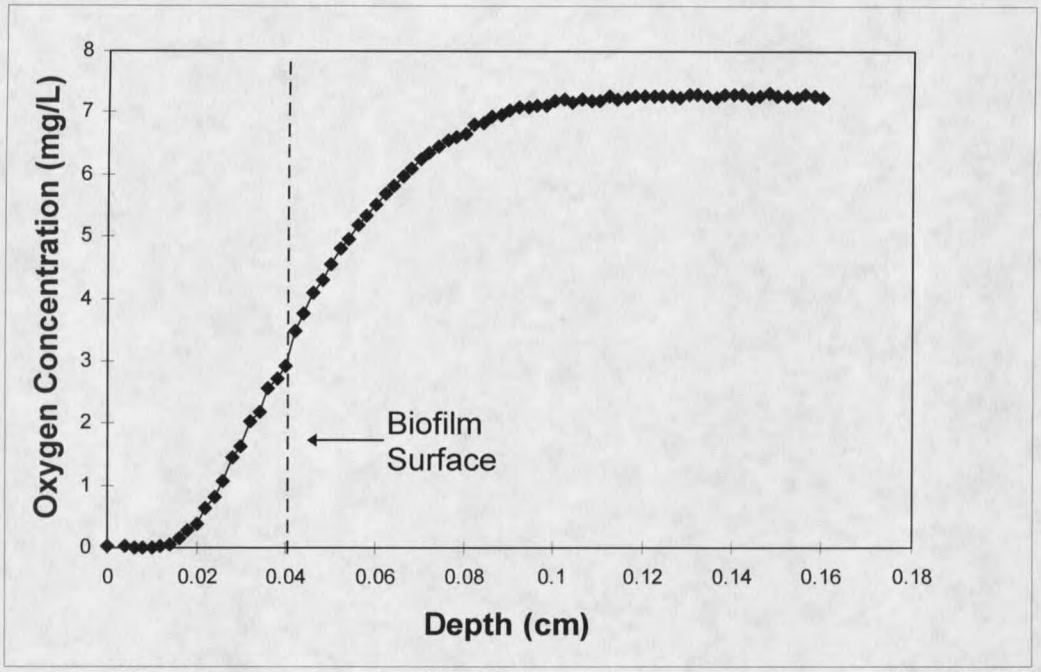


Figure 17. Dissolved oxygen profile (E) through homogeneous artificial biofilm under a low flow velocity.

Figure 18 shows the dissolved oxygen profile (F) taken 1.0 cm from the leading edge of the biofilm. The thickness of the biofilm at this point was 0.028 cm. Above x=0.09 cm the profile shows a constant oxygen value of 7.24 mg/L in the well-mixed bulk fluid. From 0.028 cm to 0.08 cm the mass transfer boundary layer that exists above the biofilm can be seen. This external mass boundary layer was 0.052 cm thick. From x=0 cm to x= 0.028 cm is the portion of the dissolved oxygen profile taken inside the biofilm. The biofilm at this location was fully penetrated with an oxygen concentration of 1.7 mg/L at the substratum.

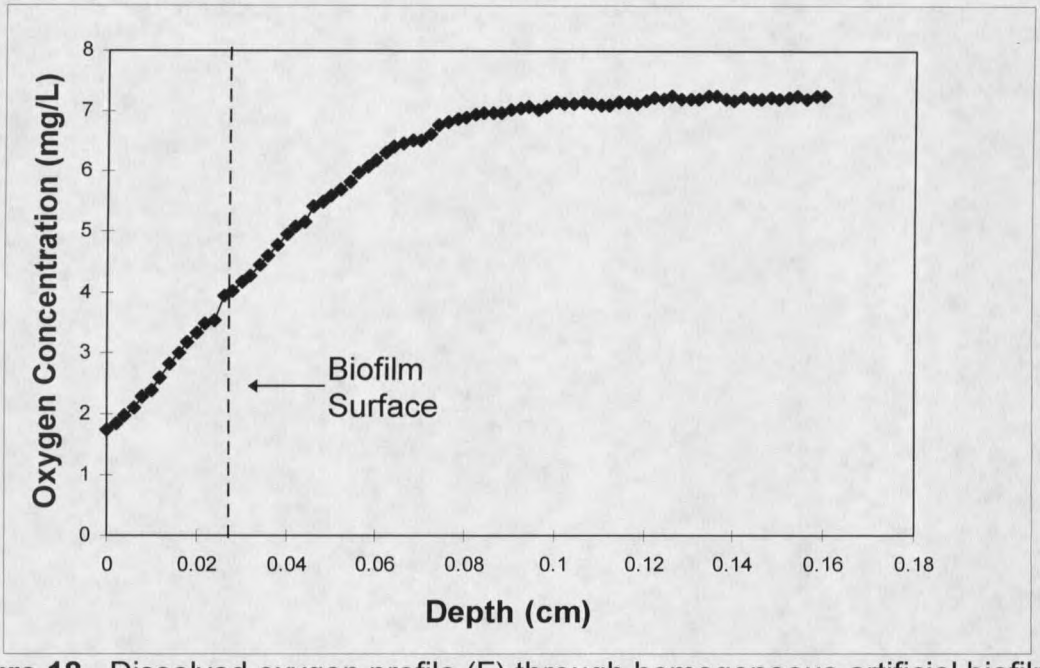


Figure 18. Dissolved oxygen profile (F) through homogeneous artificial biofilm under a low flow velocity.

Figure 19 shows dissolved oxygen profile (G) taken 0.150 cm downstream from the homogeneous biofilm. The electrode sensed a constant dissolved oxygen concentration of 7.24 mg/L until approximately 0.09 cm from the substratum. Below this point the oxygen concentration began to decrease to a concentration of 4 mg/L at the substratum.

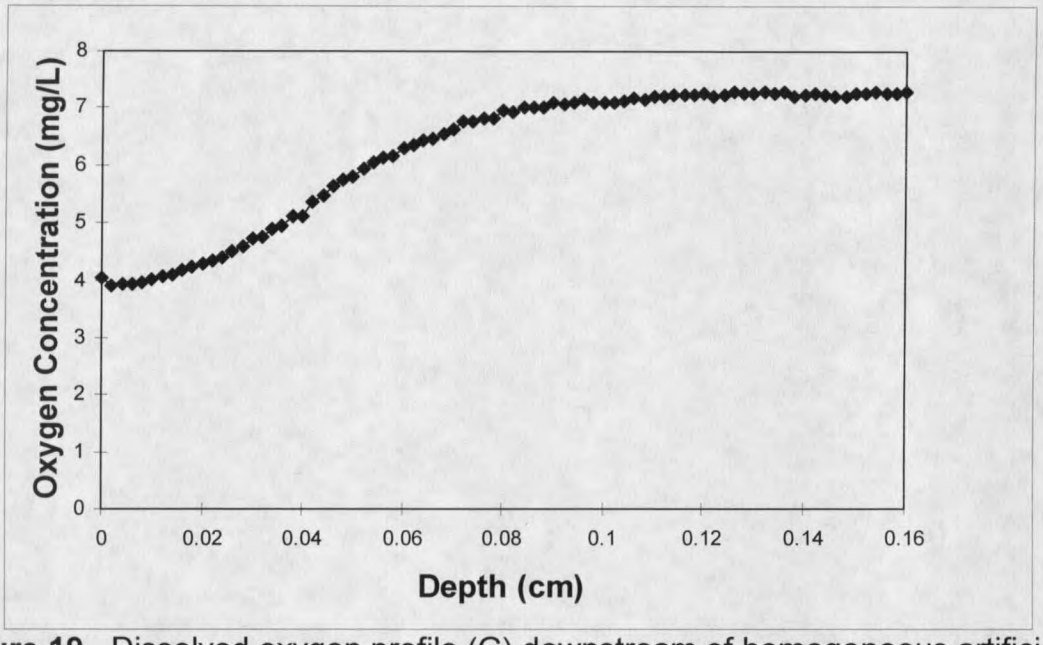


Figure 19. Dissolved oxygen profile (G) downstream of homogeneous artificial biofilm under a low flow velocity.

High Flow Velocity

Figure 20 shows the dissolved oxygen profile (A') taken 0.15 cm upstream from the biofilm. The profile maintained a value of 7.24 mg/L throughout the entire depth.

Figure 21 shows profile (B') which was taken at the leading edge of the biofilm. A constant oxygen concentration of 7.24 mg/L was measured throughout the entire depth.

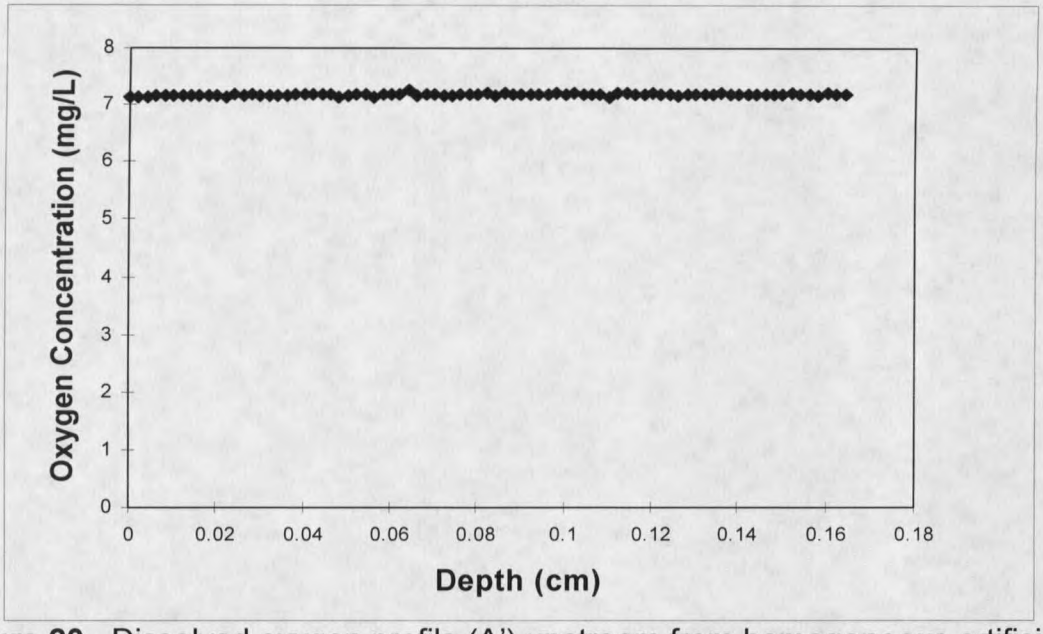


Figure 20. Dissolved oxygen profile (A') upstream from homogeneous artificial under a high flow conditions.

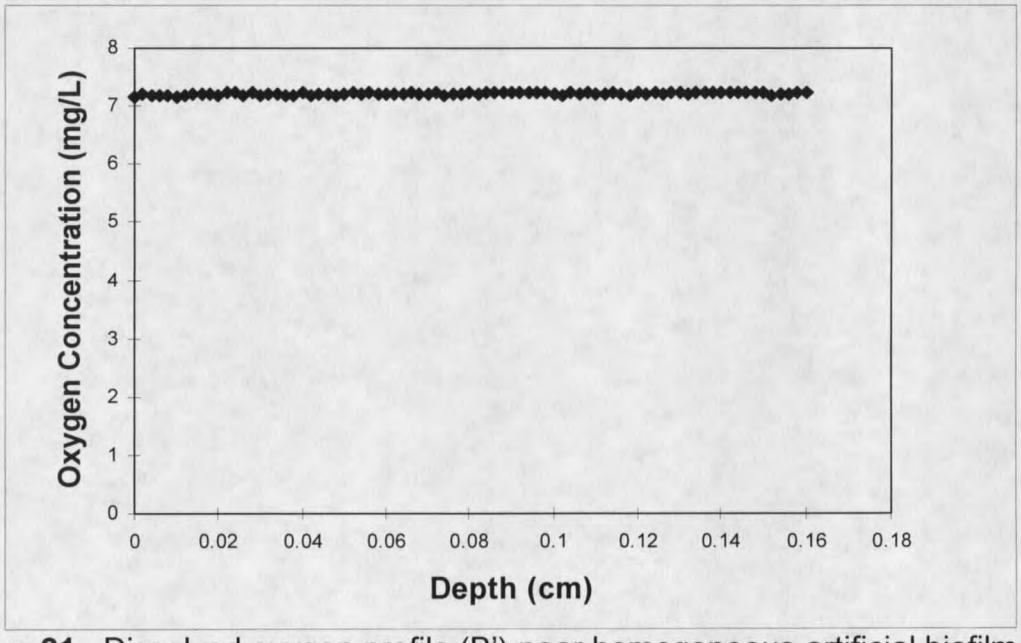


Figure 21. Dissolved oxygen profile (B') near homogeneous artificial biofilm under a high flow velocity.

Figure 22 shows the dissolved oxygen profile (C') taken 0.25 cm from the leading edge of the biofilm (point B' on figure 7). The thickness of the biofilm at this point was 0.014 cm. Above x=0.02 cm the profile shows a constant oxygen value of 7.24 mg/L in the bulk fluid. From 0.014 cm to 0.018 cm the mass transfer boundary layer that exists above biofilm can be seen. This external mass boundary layer was 0.004 cm thick. From x=0 cm to x= 0.014 cm is the portion of the dissolved oxygen profile taken inside the biofilm. The biofilm at this location was fully penetrated with a concentration of 1.3 mg/L at the substratum.

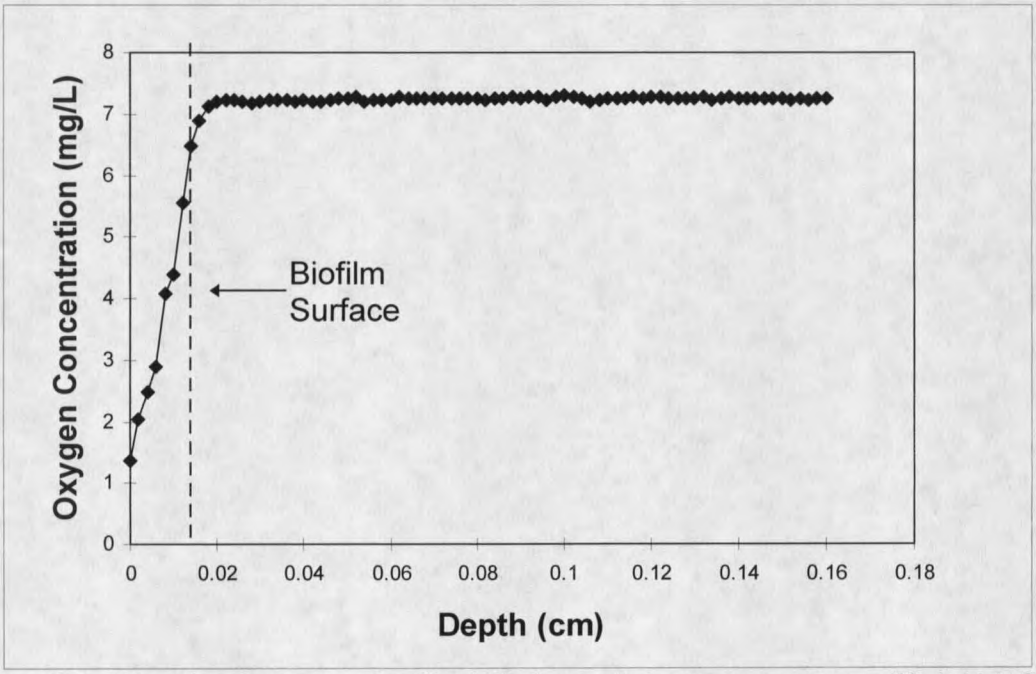


Figure 22. Dissolved oxygen profile (C') through homogeneous artificial biofilm under a high flow velocity.

Figure 23 shows the dissolved oxygen profile (D') taken 0.5 cm from the leading edge of the biofilm. The thickness of the biofilm at this point was 0.016 cm. Above x=0.022 cm the profile shows a constant oxygen value of 7.24 mg/L in the bulk fluid. From 0.016 cm to 0.02 cm the mass transfer boundary layer that exists between the bulk fluid and biofilm can be seen. This external mass boundary layer was 0.004 cm thick. From x=0 cm to x= 0.016 cm is the portion of the dissolved oxygen profile taken inside the biofilm. The biofilm at this location was fully penetrated with a concentration of 1.5 mg/L at the substratum.

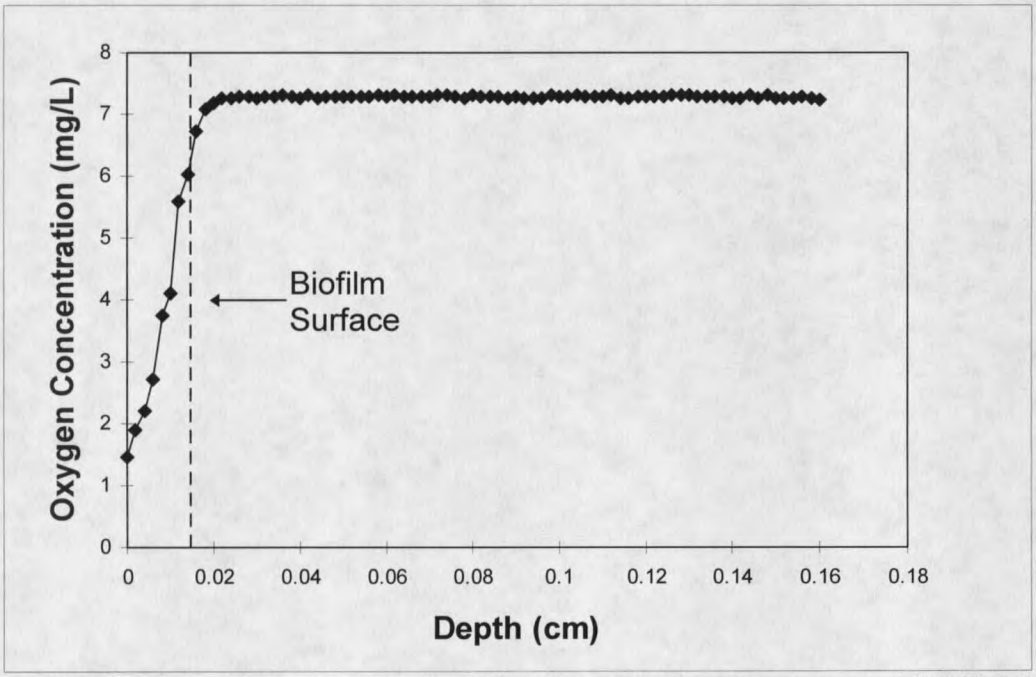


Figure 23. Dissolved oxygen profile (D') through homogeneous artificial biofilm under a high flow velocity.

Figure 24 shows the dissolved oxygen profile (E') taken 0.75 cm from the leading edge of the biofilm. The thickness of the biofilm at this point was 0.042

cm. Above x=0.048 cm the profile shows a constant oxygen value of 7.24 mg/L in the bulk fluid. From 0.042 cm to 0.046 cm the boundary layer that exists between the bulk fluid and biofilm can be seen. This external mass boundary layer was 0.004 cm thick. From x=0 cm to x= 0.042 cm is the portion of the dissolved oxygen profile taken inside the biofilm. The biofilm at this location was partially penetrated with the concentration of oxygen going to 0.0 mg/L at 0.012 cm from the substratum.

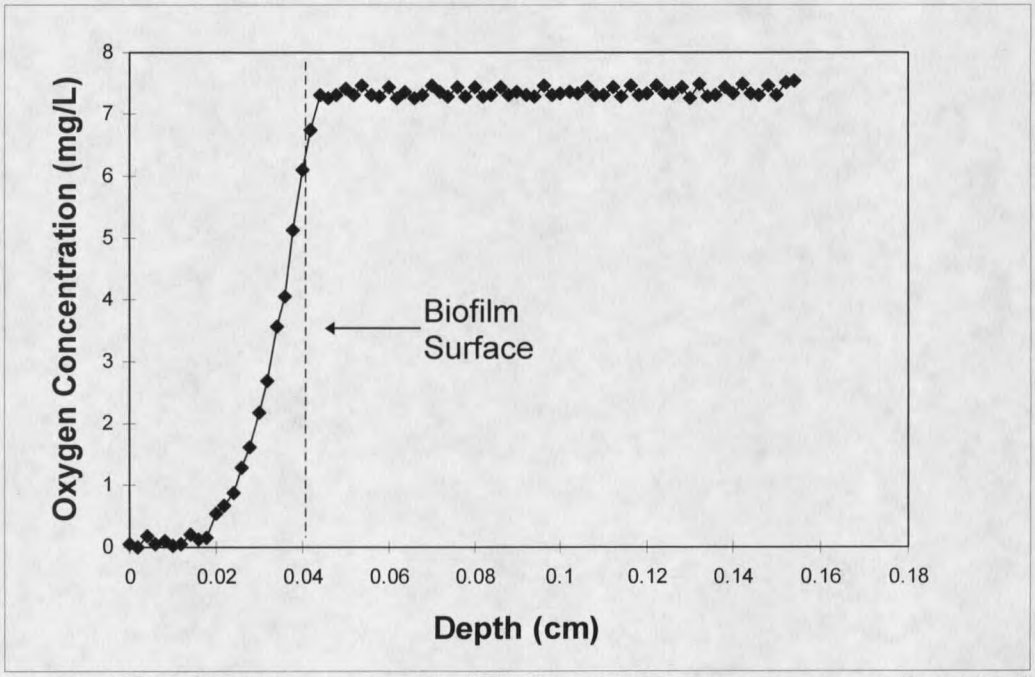


Figure 24. Dissolved oxygen profile (E') through homogeneous artificial biofilm under a high flow velocity.

Figure 25 shows profile (F') which was taken 0.75 cm from the leading edge of the biofilm. The microelectrode measured a constant oxygen value of 7.24 mg/L down to the point approximately 0.01 cm from the substratum. At this

point the dissolved oxygen concentration began to decrease to a concentration of 5.5 at the substratum.

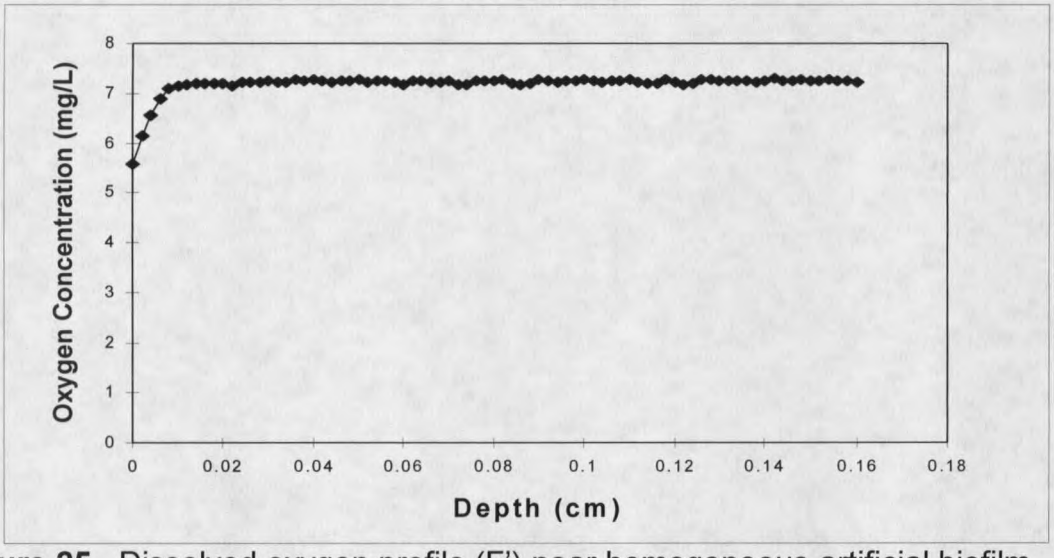


Figure 25. Dissolved oxygen profile (F') near homogeneous artificial biofilm under a high flow velocity.

Figure 26 shows dissolved oxygen profile (G') taken 0.150 cm downstream from the homogeneous biofilm. The electrode sensed a constant dissolved oxygen concentration of 7.24 mg/L until approximately 0.008 cm from the substratum. Below this point the oxygen concentration began to decrease to a concentration of 6.5 mg/L at the substratum.

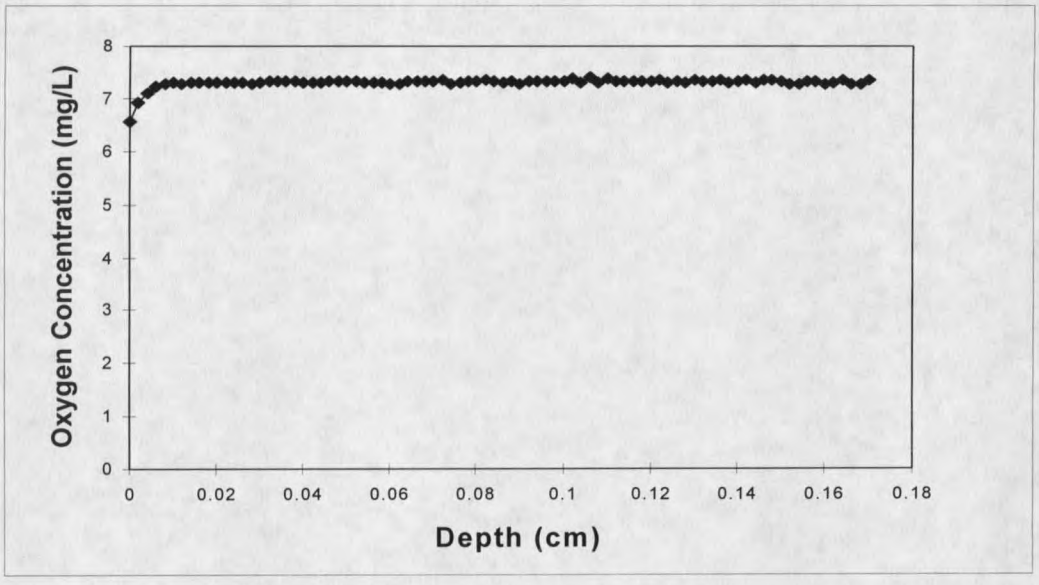


Figure 26. Dissolved oxygen profile (G') downstream from the homogeneous artificial biofilm under a high flow velocity.

MONTANA STATE UNIVERSITY LIBRARIES
3 1762 10250754 6

HOUCH
BINDERY
UTICA/OM
NE.